



CHALMERS
UNIVERSITY OF TECHNOLOGY



Cab Water-leak Detection Master's Thesis Report

Exploring Air Pressure-based Methods to Detect and Locate
Leaks in the Cabs of Volvo Trucks

Master's thesis in Production Engineering

ANDREAS JÄRLEBRATT
IBRAHIM TIMRAZ

DEPARTMENT OF INDUSTRIAL AND MATERIAL SCIENCE

CHALMERS UNIVERSITY OF TECHNOLOGY
Gothenburg, Sweden 2025
www.chalmers.se

MASTER'S THESIS 2025

Cab Water-leak Detection Master's Thesis Report

Exploring Air Pressure-based Methods to Detect and Locate Leaks
in the Cabs of Volvo Trucks

ANDREAS JÄRLEBRATT
IBRAHIM TIMRAZ



CHALMERS
UNIVERSITY OF TECHNOLOGY

Department of Industrial and Material Science
Division of Production Systems
CHALMERS UNIVERSITY OF TECHNOLOGY
Gothenburg, Sweden 2025

Cab Water-leak Detection Master's Thesis Report:
Exploring Air Pressure-based Methods to Detect and Locate Leaks in the Cabs of
Volvo Trucks
ANDREAS JÄRLEBRATT
IBRAHIM TIMRAZ

© ANDREAS JÄRLEBRATT & IBRAHIM TIMRAZ, 2025.

Supervisor: Stefan Larsson & Mikael Granbom, Volvo Group Truck Operations
Varun Gowda, Chalmers University of Technology
Examiner: Assoc. Prof. Gauti Asbjörnsson, Chalmers University of Technology

Master's Thesis 2025
Department of Industrial and Material Science
Division of Production Systems
Chalmers University of Technology
SE-412 96 Gothenburg
Telephone +46 31 772 1000

Cover: Volvo FH Aero and FH16 Aero from Volvo Group website [1].

Typeset in L^AT_EX
Printed by Chalmers Reproservice
Gothenburg, Sweden 2025

Cab Water-leak Detection Master's Thesis Report:
Exploring Methods to Detect and Locate Leaks in the Cabs of Volvo Trucks
ANDREAS JÄRLEBRATT
IBRAHIM TIMRAZ
Department of Industrial and Material Science
Chalmers University of Technology

Abstract

Water intrusion in truck cabs is a recurring quality concern, posing risks from user discomfort to component damage or failure. The current detection method at Volvo Trucks' Tuve plant relies on a water-based test that is time-consuming and resource-intensive, which makes it impractical for 100% testing coverage. This thesis investigates the feasibility of using waterless, non-destructive, air pressure-based methods to detect and locate cab leaks as an alternative to the current process. Pressure decay, together with pressure monitoring were investigated for detecting leaks, and thermal imaging as well as acoustic imaging were used for leak localization. A structured development methodology was followed, including requirement mapping, concept generation, and experimentation on pressure-based detection combined with thermal and ultrasonic imaging. The detection methods proved infeasible due to rapid pressure loss and reading overlaps between watertight and non-watertight cabs. For leak localization, thermal imaging showed limited effectiveness due to environmental sensitivity and weak thermal contrast as well as cab isolation which prevented heat from dissipating outwards. In contrast, ultrasonic imaging successfully identified several leaks with a higher accuracy. However, results were impacted by noise and surrounding disturbances which caused false positives in certain cases. Another issue was that of false positive due to harmless air leaks which were captured as potential water leaks. The study concludes that while no single method currently met all criteria for reliable implementation, ultrasonic imaging showed the most potential. Future work should hence focus on refining ultrasonic localization by addressing the existing issues. Further on, one possibility could be to investigate the option of automating the process using machine learning to aid in distinguishing critical water ingress points from harmless airflow paths to enable scalable deployment in production.

Keywords: Cab, Water Leak, Air Pressure, Ultrasonic Imaging, Thermal Imaging, Volvo Trucks, Detection, Localization, Non-destructive Testing, Production Quality

Acknowledgements

This thesis was carried out at Volvo Group Truck Operations in Tuve, Gothenburg, in collaboration with the Department of Industrial and Material Science at Chalmers University of Technology. We would like to express our sincere gratitude to our academic supervisor, Varun Gowda, and our examiner, Dr. Gauti Asbjörns-son, for their continuous guidance, constructive feedback, and support throughout the project. Their input and insights have been instrumental in shaping the academic foundation of this work. A special thanks to our industrial supervisors, Stefan Larsson and Mikael Granbom at Volvo Trucks, for their technical expertise, availability, and ongoing encouragement. Their practical perspectives and support have been crucial in enabling this work within a real production environment. We also appreciate the support and collaboration from the operators, engineers, and other staff at the Tuve plant, especially those who contributed their time and knowledge during our experimentation. Finally, we are grateful to our families and friends for their support and understanding during the course of this thesis.

Andreas Järlebratt & Ibrahim Timraz, Gothenburg, June 2025

Contents

List of Acronyms	xii
List of Figures	xv
List of Tables	xvii
1 Introduction	1
1.1 Background	1
1.2 Aim	2
1.3 Specification of the issue being investigated	3
1.4 Delimitations	3
2 Theory	5
2.1 Pressure & Flow-based	5
2.1.1 Pressure Differential	5
2.1.2 Pressure Decay	6
2.1.3 Vacuum Decay	7
2.1.4 Blower-door Fan	8
2.1.5 Mass Flow Test	8
2.2 Trace Methods	9
2.3 Wave-Based	9
2.3.1 Ultrasonic Imaging	9
2.3.2 Thermal Imaging	10
2.4 Marking based	11
2.4.1 Dye based	11
2.4.2 Soap based	11
3 Methodology	13
3.1 Mapping the Project	13
3.2 Mapping demands and requirements	15
3.3 Review of readiness	16
3.4 Requirement specification	16
3.5 Concept Generation and Screening	17
3.6 Experimentation	17
3.6.1 Pressure Testing	18
3.6.1.1 Hypothesis	18
3.6.1.2 Variables	18

3.6.1.3	Experimental Setup & Equipment	19
3.6.1.4	Procedure - Pressure Testing	20
3.6.2	Leak Identification	21
3.6.2.1	Hypothesis	21
3.6.2.2	Variables	21
3.6.2.3	Equipment and Measurement Instruments	21
3.6.2.4	Procedure	22
3.6.3	Leak Localization - Thermal Imaging	22
3.6.3.1	Hypothesis	23
3.6.3.2	Equipment and Measurement Instruments	23
3.6.3.3	Procedure	23
3.6.4	Leak Localization - Ultrasound	23
3.6.4.1	Hypothesis	23
3.6.4.2	Equipment and Measurement Instruments	24
3.6.4.3	Procedure	24
3.6.5	Concept evaluation	24
4	Results	27
4.1	Mapping demands and requirements	27
4.2	Concept Generation and Screening	29
4.3	Experimentation	31
4.3.1	Pressure Testing	31
4.3.1.1	Pressure Decay	31
4.3.1.2	Leak Differentiation Test	31
4.3.2	Leak Identification	39
4.3.3	Leak Localization	39
4.3.3.1	Thermal Imaging	39
4.3.3.2	Ultrasonic Imaging	41
5	Discussion	45
5.1	Mapping Demands and Requirements	45
5.2	Concept Development and Screening	45
5.3	Pressure Decay	45
5.4	Leak Differentiation Testing	46
5.5	Leak Identification Accuracy	46
5.6	Thermal Imaging	46
5.7	Ultrasonic Imaging	47
5.8	Production Constraints	47
5.9	Method Limitations and Future Improvements	47
5.10	Reflection & Future Research	48
6	Conclusion	49
	Bibliography	51
A	Appendix	I
A.1	2D Drawing of Pressurization Adapter	II

A.2 Leak Identification Experiment Template III

A.3 Simulated leak locations and causes IV

A.4 Requirement Specification VII

A.5 Elimination Matrix X

A.6 Leak Identification Experiment Result XII

A.7 DOE - Full Factorial Design Result XIII

A.8 DOE - 2k Factorial Design Result XVII

List of Acronyms

Below is the list of acronyms that have been used throughout this thesis listed in alphabetical order:

BIW	Body In White
DOE	Design Of Experiment
FH	Forward-control High-entry
FHX	Forward-control High-entry Xtreme
FM	Forward-control Medium-entry
FMX	Forward-control Medium-entry Xtreme
HVAC	Heating Ventilation & Air Conditioning
KD	Knock Down
ML	Machine Learning

List of Figures

2.1	Schematic showing the principle of detecting leaks using pressure differential, on the left hand side is the test object with a leak, and to the right a leak-free reference object.	6
2.2	Schematic showing the principle of detecting leaks using pressure decay, on the left hand side is the test object with a leak at the initial pressure measurement, and to the right a the test object with a lower pressure after T time has passed.	7
2.3	Schematic showing the principle of detecting leaks using vacuum decay, on the left hand side is the test object with a leak at the initial pressure measurement (vacuum), and to the right a the test object with a higher pressure after T time has passed.	7
2.4	Illustration schematic over the mass flow test showing the different components and general function.	8
2.5	Illustration schematic over trace methods.	9
2.6	FLIR Si2-Pro Acoustic Camera [49].	10
2.7	FLIR E96 Thermal Camera [56].	11
3.1	Development funnel outlining the screening and different phases included in the methodology for the project, whereas the gray-outed areas were conducted by the project partner Volvo Trucks. Modified and adapted from [60].	14
3.2	The different phases from the development funnel described, with respective steps and screens. Modified and adapted from [60].	14
3.3	Main test setup used for pressurization and experimentation.	19
3.4	CAD render of adapter module used for pressurization. Further and additional specifications of the adapter can be seen in the 2D drawing found in <i>Appendix A.1</i>	20
4.1	Scatterplot showing average pressure levels for watertight and non-watertight cab at different temperatures of the injected air for the power level 50%.	32
4.2	Scatterplot showing average pressure levels for watertight and non-watertight cab at different temperatures of the injected air for the power level 75%.	33
4.3	Scatterplot showing average pressure levels for watertight and non-watertight cab at different temperatures of the injected air for the power level 100%.	33

4.4	Showing the pressure achieved at different temperatures, at power level 50%, for watertight and non-watertight cabs at two different experimental runs.	34
4.5	Showing the pressure achieved at different temperatures, at power level 75%, for watertight and non-watertight cabs at two different experimental runs.	35
4.6	Showing the pressure achieved at different temperatures, at power level 100%, for watertight and non-watertight cabs at two different experimental runs.	35
4.7	Pareto chart showing the standardized effect for the given significance level of 0.95.	36
4.8	Main effect plot showing the mean of pressure given changes in temperature, power level and water tightness.	37
4.9	Pareto chart showing the standardized effect for the given significance level of 0.95 when only evaluating the two lower temperatures, and two highest power levels.	38
4.10	Main effect plot showing the mean of pressure given changes in temperature, power level and water tightness for two levels of temperature and power level.	38
4.11	Showing the relative pressure loss of different leak points in comparison to maximum pressure, achieved before the leak was created, for two different experimental runs.	39
4.12	Thermal image showing the ambient disturbances when taking a picture at a wider angle.	40

List of Tables

3.1	Variables during pressure experimentation.	19
3.2	Variables during pressure experimentation.	22
4.1	Performance requirements with respective number extracted from the full specification.	28
4.2	The remainder of the defined requirements.	28
4.3	The different sub-functions and their respective sub-solutions used for in the morphological matrix in order to generate concepts from solution combinations.	29
4.4	The different solutions generated after combining the sub-functions in a morphological matrix.	30
4.5	Final Concepts prior to experimentation.	30
4.6	Thermal Images from various points of interest before and after temperature delta.	41
4.7	Ultrasonic Images from various points of interest.	42

1

Introduction

This chapter introduces the problem briefly through presenting background information as well as defines the aim, limitations, and research questions of the project.

1.1 Background

Each year, millions of heavy-duty trucks are manufactured and integrated into the global transportation network. In 2024 alone, approximately 6.4 million trucks were produced worldwide and this number is projected to grow steadily with an annual production expected to reach up to 7.4 million trucks by 2030 [2]. The trucks are often bought at a significant cost to the customer, hence its also bought with an expectation of quality. Even though companies follow different strategies, a drive for continuous improvement of quality is important, as it not only can increase customer satisfaction but also reduce cost in terms of customer claims. Quality has many different dimensions, from visual and comfort, to safety. A quality risk associated with all dimensions and is not only limited to heavy trucks, is that of water leaks.

A passenger cabin (cab) of any vehicle is expected to be water tight and no water should leak into the inside. There are a number of risks associated with water intrusion into the cab, the least severe being user discomfort, and the most severe being flooding of the cab or failure of electrical components, both of which can result in fatal accidents on the road [3]. To minimize this, it is crucial to have a water leak detection process as part of the quality check in vehicle manufacturing, thus securing the cabin tightness before it reaches the customer. In addition its important to have an implemented detection process that has the ability to match the production pace and can be used on all cabs within the desired cycle time.

The Volvo Trucks plant in Tuve, Gothenburg, produces various variants of the company's model range, together with the possibility of a wide variety and possibility of customization based on the customers needs. However, the main chassis and foundation of which the adaptation is built upon is limited to a certain number of models. Among the models produced in Tuve are the smaller FM/FMX model, the larger FH/FHX model with its variations FH16, FH Aero (extended front) and FH XXL. Besides this the plant also produces its FM/FMX model in a crew cab variant (crew cabs are modified cabs with an extension to fit additional persons behind the

driver, e.g., used for firetrucks), which makes up a small percentage of the trucks produced, and also deviates in terms of assembly process compared to the previously mentioned models.

The current water-tightness required for the cab is defined as "*Total water-tightness with no leaks permitted for basic body when complete with sealing compound, cover plates, body fastening nuts, and plugs*" [4]. Internal historical Volvo specific quality data shows that leaks originate from a number of causes, whether a missing screw, a badly fitted plug, or the inconsistent application of glue compound (personal communication, January, 2025). The data also indicated that there are quality issues in the process that ultimately lead to water leakages, and if those are dealt with, the leakage risk into the cab would be considerably minimized. It is crucial to have quality checks in place to guarantee product quality [5]. The current process of testing, performed in the designated facility at the end of the cab production line, sprays the entire cab with water at a rate of 500 liters/minute at a pressure of 600 kPa, and for a minimum of 10 minutes for cabs produced on the line, after which the operator checks risk areas for any leaks [3]. This process simulates various operational conditions, the worst of which is 800mm rain [4], [6].

This process is far from optimal, since the process in itself poses a risk of damaging the interior of the cab if a leak does occur and components would have to be repaired or replaced in such cases. The process is also time consuming as cabs must be transported to and from the test rig, they must then be prepared, tested, and checked. This means that the total number of cabs that can be tested on any given day is only a fraction of the total produced, all of which ideally should be tested. Even that fraction can vary depending on the overall availability of the testing station which is affected by a number of factors. For example, the number of cabs that need manual adjustments, and the need to rerun the test in case of a leak being found and adjusted, which consumes the total available time for testing other cabs (personal communication, January, 2025). This naturally increases the risk of having defective cabs, or cabs with a high risk of leakage, reach their final customer. However, since the water test has a cycle time of at least 10 minutes which is almost triple the takt time, it is a vast challenge to test 100% of the produced cabs. These reasons give rise for a need to investigate alternative testing solutions.

Even though the automotive is one of the biggest industries in the world [7], the research and innovation of the leakage tests for cabins is limited. Companies have stayed with the classical water-test for the cabins as it yields an accurate result [8], [9], however the previous mentioned risks are still present. Meanwhile the research and innovation for leakage testing of other parts in the trucks and cars has continued as for example, pressure and tracer gas testing of engine blocks [10], and ultrasound for testing windscreen bonding quality [11].

1.2 Aim

The aim of this project is to investigate the possibility and feasibility of using a waterless air-pressure based and non-destructive test method to detect the presence

of and locate possible water intrusion into truck cabins. In addition, the project aims to design, build and acquire the relevant equipment for experimentation and testing of the feasibility of the test method.

Additionally, the project aims to identify stakeholders, gather requirements, design the process and equipment that fulfills the requirement, and verify the potential and accuracy of the test method.

1.3 Specification of the issue being investigated

This section presents the questions which this project aims to answer.

Research Questions:

1. Can a waterless test method effectively detect water intrusion in truck cabs with accuracy comparable to the current water testing method?
2. How can the new method reliably detect and locate the most common causes of water leaks in cabs?
3. What equipment and tools are required to implement the new process in a scalable manner?

1.4 Delimitations

The following points were considered out of scope for this project:

1. This study was limited to the variants produced in the Tuve plant i.e. FM, FH, FH16 and FH Aero.
2. The crew cab variant was not be investigated.
3. The project focused solely on water leaks, excluding other types of ingress or moisture penetration.
4. Testing the new method on non-standard or prototype cabs was not included.
5. Comprehensive cost analysis beyond the initial implementation was not part of the study.
6. Environmental factors (e.g., extreme weather simulation) that may affect water intrusion were not considered, besides those specified in the Volvo Group EMEA-P-069 Water test specification.

2

Theory

Water leak detection is a critical aspect of ensuring vehicle quality, durability, and customer satisfaction. Various methods have been developed to identify and mitigate leaks, each with its advantages and limitations. This chapter, as part of the literature study, explores different methods used in leak detection -ranging from pressure and flow-based methods to more advanced wave-based methods. The objective is to analyze these methods to understand their effectiveness and applicability while establishing a foundation for an optimized and scalable leak detection strategy that aligns with modern automotive manufacturing standards. Additionally, this section presents the initial literature review conducted to gain insights into various techniques used across different industries, providing introductory information on existing applications.

Although the literature study explores methods from different application, the focus is not on integrating or combining these methods to enhance detection accuracy and efficiency. Instead, the insights gained from this study are for understanding different methods and their applications since the focus will mainly be on methods where compressed air is the main medium for detection. This approach aids in the development of a new method that leverages the strengths of existing approaches while addressing their limitations.

2.1 Pressure & Flow-based

This section outlines a range of air-based leak detection methods that rely on either pressure variations or airflow measurement to identify the presence of leaks. These techniques differ in sensitivity, application suitability, and operational complexity. Furthermore, each technique offers distinct advantages and limitations depending on the test object's characteristics and the intended use case. By understanding the principles and trade-offs of each approach, a more informed selection can be made to match specific testing demands further on in the development phases.

2.1.1 Pressure Differential

Air is a medium that can be utilized easily to identifying leaks by using air pressure differences or air flow rates. There are multiple ways pressure and air flow can be utilized for leak detection, a few of which are discussed in this section. Air pressure

is used to identify leaks by putting the system into a pressurized state in comparison to the environment around, making it more likely for a leak to occur. [12]. However, there are specific methods that differ and are utilized depending on the application. A well established method utilized for identifying leaks is to measure the differential pressure [13] where the static pressure of a pressurized test object is compared to that of leak-free reference to identify the presence of a potential leak [14], a schematic of this method can be seen in *Figure 2.1*. This method offers accurate detection of leaks provided the quality, or tightness level, of the reference object is guaranteed. However, the application of this method is limited to mainly tight and relatively simple systems such as pressure vessels.

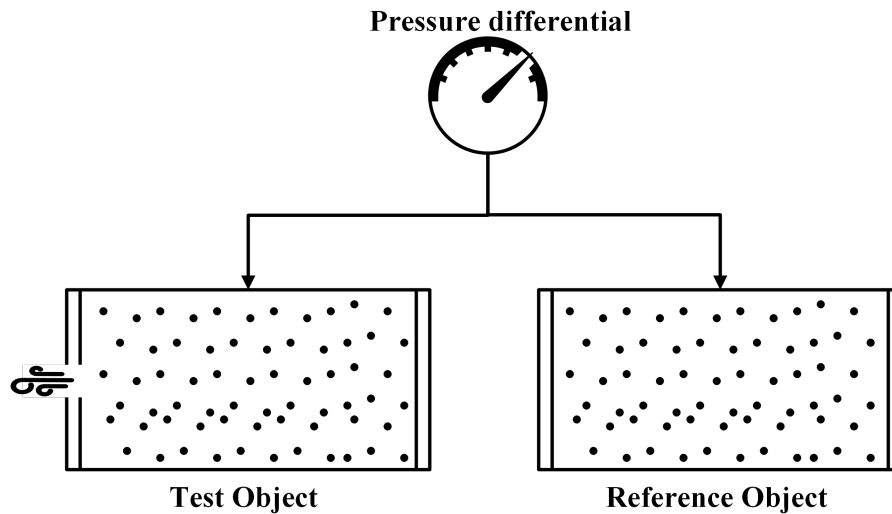


Figure 2.1: Schematic showing the principle of detecting leaks using pressure differential, on the left hand side is the test object with a leak, and to the right a leak-free reference object.

2.1.2 Pressure Decay

Similarly, a widely adopted method is *pressure decay*, used to detect leaks by pressurizing a test object to a set stable pressure then measuring the drop in internal pressure over a certain period of time, a schematic of the method can be seen in *Figure 2.2*. This approach is effective when working with smaller leaks through monitoring the pressure decay curve of the system [15]. This method is particularly useful for primarily tight systems that require non-destructive testing or even real-time data acquisition and analysis [16]. In contrast, one of the drawbacks using the pressure decay method is that the result is easily affected by temperature imbalances as it affect the overall pressure and can mimic the presence of leak [13]. Coupled with this, the method is also only suitable for detecting the presence of a leak and not locating it, as the pressure indication is for the overall state of the system. Another possible drawback is that a system in an over-pressure state leaks outwards where water intrusion in real situations is into the system, which means that this may not simulate the real situations the study is after since the leak flow would be reversed.

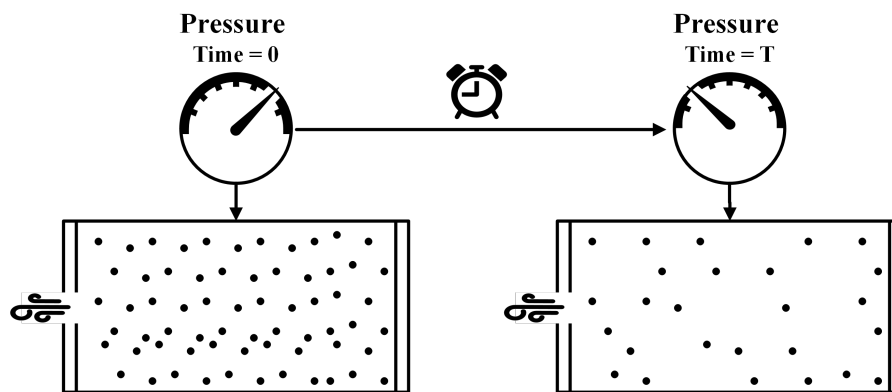


Figure 2.2: Schematic showing the principle of detecting leaks using pressure decay, on the left hand side is the test object with a leak at the initial pressure measurement, and to the right a the test object with a lower pressure after T time has passed.

2.1.3 Vacuum Decay

Vacuum decay is a method similar to *pressure decay*, but is performed in an inverse manner. This is where the system is put into an under-pressure or near vacuum state (depending on structural pressure constraints) and the progressive decay of the under-pressure state is monitored over time to detect the presence of a potential leak into the object, a schematic of this method can be seen in *Figure 2.3*. This method is mainly used for testing different types of packaging for leaks, and has been successful in detecting leaks as small as $5\mu\text{m}$ in diameter [17]–[19]. However, similar to pressure decay, it is susceptible to temperature variations which needs to be accounted for [20]. This method is most suitable for simpler test objects like packages, tanks, etc. and not complex structures as the vacuum can close off potential risk areas.

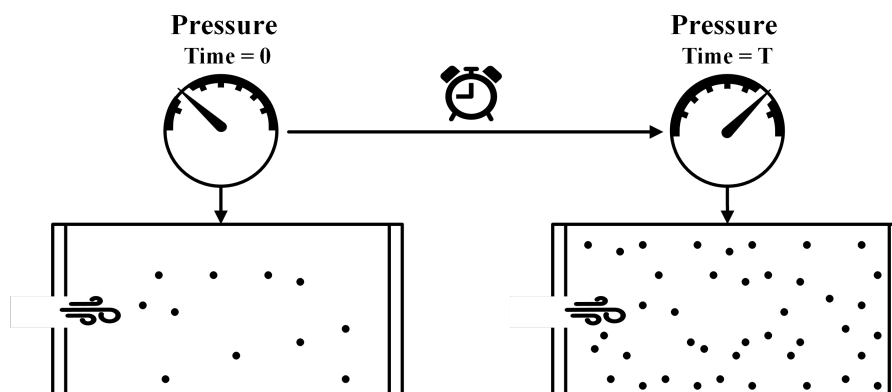


Figure 2.3: Schematic showing the principle of detecting leaks using vacuum decay, on the left hand side is the test object with a leak at the initial pressure measurement (vacuum), and to the right a the test object with a higher pressure after T time has passed.

2.1.4 Blower-door Fan

Another method that utilizes the flow of air and pressure differences called the *Blower-Door Fan* method. This method is mainly used for measuring air leakage rates in buildings by creating pressure differences between the inside and outside and the airflow required to maintain the pressure difference is measured to determine the building's air leakage rate [21]–[23]. Although the main application for this method is buildings, a study has been conducted on school buses and showed potential for measure leaks in vehicles [24], it has also been applied for testing aircraft cargo hold leakages [25]. This method gives accurate results and provides real-time quantitative data at a relatively low cost, as well as being versatile and adaptable for different applications [21], [26], [27]. It is worth noting that this method is more effective when combined with other detection methods to more accurately locate the leaks, such as thermal imaging [27].

2.1.5 Mass Flow Test

Finally, there is a method where air flow is main test medium rather than air pressure, which is called the *Mass Flow Test*. The test object is pressurized to a predetermined level, usually as a reference object, and the fluid flow is measured to detect leaks. The setup of this method can be seen in the schematic in *Figure 2.4* This method requires a sealed system, and once stabilized, the flow rate is monitored to identify any deviations that indicate a leak [28], [29]. This method is suitable for applications where high detection accuracy is needed, as it is capable of detecting leaks as small as 0.02sccm [29]. It is also versatile and can be adapted to different applications such as aerospace shuttle systems, while also providing the opportunity to automate the process [30]. On the other hand, the high accuracy and potential comes at the cost of set-up complexity and high equipment costs [28], [29]. The process is also sensitive to environmental factors and the calibration is time-consuming, making it less than ideal for high paced environments like factories, as well as the fact that a truck's cabin is nowhere near as air-tight or sealed as this test requires [29].

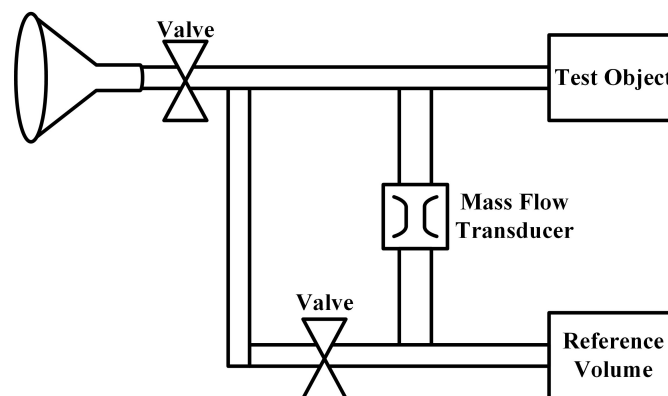


Figure 2.4: Illustration schematic over the mass flow test showing the different components and general function.

2.2 Trace Methods

Air leak testing using trace methods involves detecting leaks by introducing trace gases such as hydrogen (H_2) [31], helium (He) [32]–[34], or carbon dioxide (CO_2) [35], into a sealed environment and monitoring their escape. Smoke is also used in certain applications, allowing for visual confirmation of leaks [36]. The presence of these trace gases outside the sealed environment can be monitored using sensors, mass spectrometers, or sniffers, ensuring precise detection of even the smallest leaks [31]. An illustration of the method can be seen in *Figure 2.5*. This method is especially useful in industries where manufacturing precision is crucial.

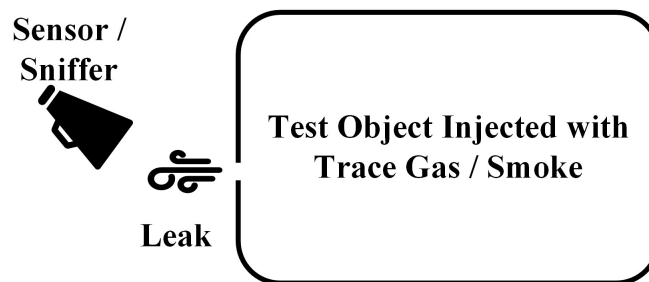


Figure 2.5: Illustration schematic over trace methods.

While trace gas methods for air leak testing offer high detection sensitivity and accuracy, they also come with some drawbacks. One major drawback is the need for specialized equipment, which can be expensive and require skilled operators to use properly [37], [38]. Additionally, certain trace gases, like hydrogen (H_2), can be hazardous if not handled carefully, posing safety risks, particularly in confined spaces or environments with high flammability [39]. Another issue is the potential for false positives or interference if the test area is contaminated with substances that can affect sensor readings [40]. Finally, these methods can be relatively time-consuming and may not be suitable for testing large volumes of products quickly, making them less ideal for high-throughput production environments.

2.3 Wave-Based

This section provides an overview of wave-based leak detection methods, focusing on the use of ultrasound and thermal imaging. These techniques rely on sound and infrared waves to identify the presence of leaks and can be used in various industrial applications. The following section describe how each method works and their typical use cases.

2.3.1 Ultrasonic Imaging

A method for detecting leaks is by utilizing the existence and behavior of ultrasound waves [41]. *Ultrasonic detection* is a method used mainly for pneumatic systems and electrical systems. There are multiple ways this can be done, the first of which

is placing an ultrasound emitter on either side of the barrier and an ultrasonic detection device on the other side [42]. The second method is where ultrasonic waves are formed when air passes through holes, and the waves are then detected with an ultrasonic detector, which helps identify and locate the leaks [43]. The detector can be a microphone coupled with a headset where the ultrasonic waves detected are conveyed into the headset to be heard by the tester. Alternatively, an ultrasonic camera which detects the ultrasonic waves by utilizing a sensor array that can map the sound to imaging can be used - allowing for visual display and identification of the leaks' [44]. An example of an ultrasonic camera is displayed in *Figure 2.6*. Ultrasonic detection is known for its relatively high sensitivity [42], and producing accurate results especially when paired with certain machine learning (ML) algorithms to aid with classifying results [45]. This method is also very suitable for noisy environments as it filters out most unwanted frequencies [46]. Filtering is however not perfect and results can be affected by background noise depending on the environment, thus increasing the results for false positives, especially if no advanced filtering algorithms are employed [45], [47]. Another drawback is the cost of high-quality sensors and transducers, especially if applied at a larger scale [48].



Figure 2.6: FLIR Si2-Pro Acoustic Camera [49].

2.3.2 Thermal Imaging

Thermal imaging is technology that utilizes infrared cameras, like the one shown in *Figure 2.7*, to detect temperature variations, which allows for the identification of fluid leaks in different systems such as pipes, roof, or building structures. This method is used in industries like automotive manufacturing and oil and gas to identify various types of leaks to enhance operational efficiency and safety [50], [51]. Visualizing temperature discrepancies allows for accurate and rapid leak detection [52]. This method is efficient and accurate for testing leaks around parts like sunroofs, windows, and doors [50]. Depending on the size and location of the leak, thermal imaging may be more or less accurate in detecting leaks as it relies on the interpretation of the images which can produce false positives or reduce the accuracy when detecting smaller leaks [53]. However, advanced techniques such as deep

learning and complex algorithms have been developed and can be utilized to improve and automate detection accuracy [54], [55].



Figure 2.7: FLIR E96 Thermal Camera [56].

2.4 Marking based

This section outlines leak detection methods that use visual markers to identify potential leak paths. These approaches, including dye-based and soap-based techniques, rely on physical indicators to reveal the presence and location of leaks. Marking-based methods are often straightforward to apply and require minimal equipment, making them useful in certain contexts, especially for simpler systems or initial inspections. The following sections describe how each method works and the typical situations in which they are applied.

2.4.1 Dye based

The marking based leak detection is manual and non-technical method. An example of this is the *penetrant dye test*. This method involves the forced introduction of a florescent dye to the test object by placing it under pressure for a few hours. This forces the dye to make its way through leaks and its flow is then traced using an ultraviolet lamp, thus showing the location of any possible leaks [57]. In many cases, the disassembly of the object may be required to observe inside it, making this method more suitable for simpler objects [57]. Another drawback that is immediately noticed is the risk of staining interior components, and this method requires post cleaning of the test object.

2.4.2 Soap based

When a leak is induced using an overpressure, this leak can be located simply by spraying a thin layer of soap solution on and around areas where the leak could come from and observe the formation of bubbles [58]. A leak is indicated by the formation of larger, rapidly formed bubbles which show the air flow coming from

the suspected area [58]. This method is widely used in, mainly in gas pipes and and vehicle Heating, Ventilation, and Air Conditioning (HVAC) systems. Using soap for detecting leaks is simple and cost-effective in the sense that no equipment is needed besides that for pressurizing the system [59]. However, it is not the most accurate method out there and is time-consuming for larger applications where there are many possible leak points [59].

3

Methodology

This chapter presents the methodology utilized during the span of the project, ranging from data collection, mapping of requirements and wants, to concept generation, selection and experimentation. The methodology was designed in such a way to investigate the research problem in a systematic manner using quantitative and experimental approaches for data collection, in combination with what has been presented in *Chapter 2*.

3.1 Mapping the Project

Due to the reasons mentioned in *Subchapter 1.1*, as well as the recent product launches for the North American market, Volvo has been working on investigating alternative solutions for identifying water leaks in order to be able to reliably test 100% of produced cabs. As part of this global initiative, the organization in the Tuve plant have been responsible for investigating compressed air-based methods, which is where this project stems from. This special situation affects the overall process in such a way that concept generation will be limited to working with methods that utilize compressed air as the main medium, and multiple concepts will be tested to check for feasibility.

Wheelwright [60] describes one appropriate approach towards project structures in this way using his model of *Innovative and Focused development funnel*. The approach describes the project as it is taken through various screenings (*Screens*) where concepts are relatively quickly eliminated to reduce the number of alternatives compared to a more classical project development methodology. Wheelwright describes this as putting *all-the-eggs-in-one-basket* due to the risk of neglecting solutions, however with the benefit of saving time and resources. The approach is visualized as seen in *Figure 3.1*, however for this project, with the modification and addition of an initial phase - *Pre-study and Initial Research* which refers to the first screening and technology search done by Volvo.

The development funnel is further shown with a description to each part in *Figure 3.2*. The first phase pre-study and initial research was, as mentioned in previous paragraph, an extensive scan of all types of leak detection methods executed by Volvo. Based on this and the preliminary findings, Volvo then conducted an initial screening to define the scope of the subsequent phases, after which this project

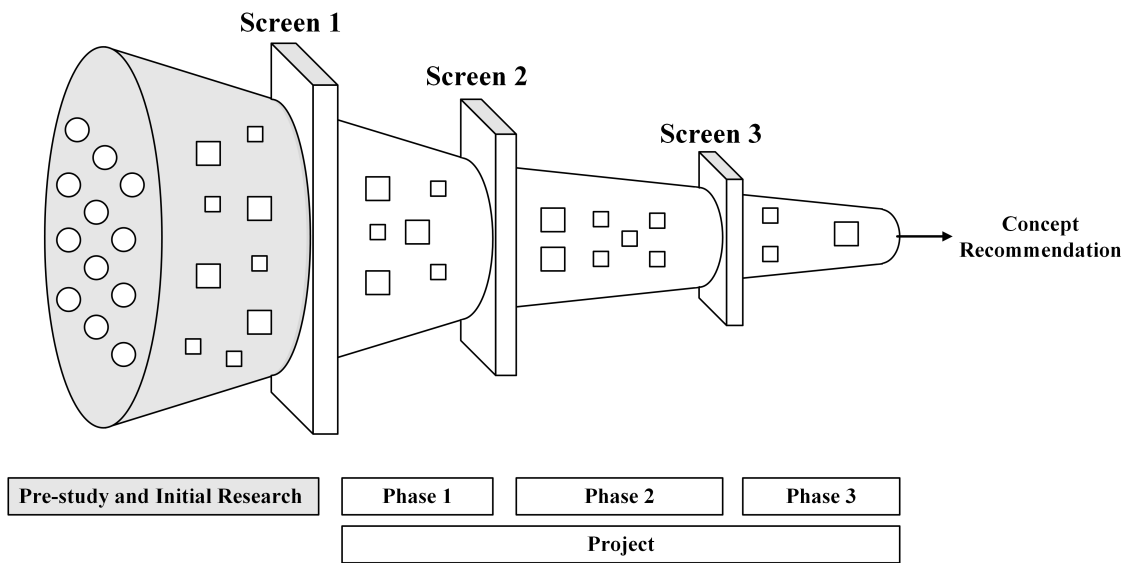


Figure 3.1: Development funnel outlining the screening and different phases included in the methodology for the project, whereas the gray-outed areas were conducted by the project partner Volvo Trucks. Modified and adapted from [60].

Pre-Study and Initial Research	Extensive scan of leak methods and solution concepts.	
Screen 1	Decision and selection of relevant methods, concepts and set project scope.	
Phase 1	Product and process generation and concept development.	Search for existing technologies. Mapping demands and requirements.
Screen 2	Review and readiness evaluated. If found viable the concept is moved on.	
Phase 2	Detailing of proposed project bounds and required knowledge.	Specifying demands and requirements. Concept generation.
Screen 3	Concepts are given go/no-go based on fulfilment of requirements.	
Phase 3	Focused development and evaluation.	Prototype building. Experimentation.

Figure 3.2: The different phases from the development funnel described, with respective steps and screens. Modified and adapted from [60].

assumed responsibility for further development. Following this, the methodology for this project started with an initial search for existing technologies within the limits of pressure based alternatives for leak detections of which the result, as previously mentioned in the theory, *Chapter 2*. Following this a mapping of demands and requirements was performed, the procedure for this is further described in *Subchapter 3.2*. Subsequently the project passed through the second screen, where a review of the readiness and applicability of the found technologies was done.

Thereafter, the second phase initiates a more detailed approach towards the development, and a requirement specification was established with quantifiable measures for the concept, which are to be used in the evaluation - more on this in *Subchapter 3.4*. This phase also included a more extensive concept generation of the remaining concepts which in the final screening got further evaluated for a go/no-go decision before the final phase - a greater description of this phase is found in *Subchapter 3.5*. The third and final phase includes focused development and evaluation of the remaining concepts. For this project this meant extensive testing and experimentation. To make this possible it first required that prototypes was build and testing equipment acquired. This was then followed by the experimentation and the analysis of the results, more on the exact methodology regarding this is found in *Subchapter 3.6*.

3.2 Mapping demands and requirements

To ensure that the redesigned leak test aligns with operational expectations, a mapping of the demands and requirements was conducted. The objective was to identify key challenges and new requirements. Those requirements are divided into two categories. The first being performance/functional requirements for the test to be accepted for further development, and the second being potential requirements for a functional process where more factors are considered. Furthermore, a requirement was defined as a condition that must be fulfilled, whereas a demand was considered a stakeholder preference that adds value to the solution but is not essential for its completion. By incorporating these factors early in the process the requirement specification could be refined to better support production needs and enhance the test's effectiveness. The first category is what was considered during the course of the scope of this project.

The mapping process was carried out in close collaboration with key stakeholders, including operators, engineers, and quality assurance personnel through several discussions in order to gather insights and understanding of existing flaws and desired improvements of the testing method. This phase also served as a foundation for integrating customer demands into the requirement specification. The insights gathered from this process can help to ensured that the final solution not only addressed the technical performance requirements but also aligned with operational constraints and ergonomic considerations, with the goal of improving both test efficiency and overall product quality.

3.3 Review of readiness

The review of readiness is done at the second screen of the development funnel following the mapping of demands and requirements. This phase involves an initial qualitative evaluation of the previously generated concepts, not through strict benchmarking against a formal requirement specification, but by assessing their general compatibility with the intended implementation environment and the strategic direction of Volvo's manufacturing based on the performed mapping. The goal of this is to identify whether a concept demonstrates a sufficient potential to proceed to a more detailed development, based on feasibility, integration capability, and alignment with the mapped demands and requirements.

The review is as mentioned in previous paragraph based on the insights collected during the mapping of demands and requirements. By evaluating each concept against these broader expectations defined during the mapping, such as detection accuracy and takt time compatibility, the review helps in ensuring that unsuitable solutions are filtered out early. The benefit of utilizing this approach is that it allows for a more focused and efficient development in the upcoming steps, by allowing for the direction of resources towards solutions that not only are technically promising but also are appropriate for the contextual setting in which the concept are to be used.

The review of readiness is, like the mapping of demands and requirements, conducted in collaboration with key stakeholders and engineers etc., whose perspectives provide valuable input on whether a concept meets the demands of the organizations goals. This screen serves as a bridge between the previous more exploratory phase and the upcoming, more formalized evaluation easing the balancing between innovative efforts and practical implementation conditions.

3.4 Requirement specification

In order to move from general expectations to an acceptable solution and conforming design each mapped demand and requirement needed to be quantified into measurable values. This step ensures that the specification not only is descriptive but also verifiable, thereby allowing for structured testing and evaluation in the following phases of the development funnel. This process was, once again, carried out in collaboration with the different key stakeholders and operational personal to ensure technical feasibility and relevance to the real-world production setting. Each requirement was discussed to determine appropriate benchmarks based on the required capabilities and technical requirements within the company. Furthermore to support prioritization, each demand was assigned a rating from *1* to *5*, where *5* represents the highest priority and *1* the lowest.

Quantifying the requirements also supports the development process by establishing clear pass/fail criteria. This contributes to more efficient prototyping and iterations as different concepts can be assessed against quantified values. Furthermore, the measurable values for each demand and requirement allows for traceability and

transparency throughout the development as potential benefits, drawbacks can more easily be justified as trade-off given there is a measurable value to compare against.

3.5 Concept Generation and Screening

The concept generation phase was conducted systematically by drawing inspiration from previous results, this being the findings from existing solutions, customer requirements and functional demands. This phase aimed to develop potential solutions by exploring a range of ideas and solutions before narrowing them down to the most promising concepts.

To facilitate this process multiple idea-generation techniques were used. Brainstorming sessions were held to generate a foundation of ideas, in order to encourage creativity and out-of-the-box thinking the majority of defined requirements were not considered. Workshops were conducted with an external party to refine these ideas and allowing for collaborative discussions where feasibility, practicality, and potential challenges were brought into focus. The reason for including an external party was to get non-biased input and ideas to the functions. Additionally, a morphological matrix was used to systematically break down key solutions into their fundamental parts, enabling structured recombination of different solutions to form new concepts.

By utilizing these techniques, it was ensured that the concept generation process was both creative, feasible and structured, allowing for a comprehensive exploration of possible improvements. This approach helped in identifying viable solutions that possibly could enhance the efficiency without utilizing water.

Before the last phase of the development funnel the third screening process took place, this with regards to the fulfillment of the requirement specification. Here the concepts were evaluated against the established requirements and were given either a go- or no-go decision in terms of continued development. To perform this evaluation an elimination matrix was used, where the concepts were given either a *Yes*, *No* or *'?'*, in terms of fulfillment, fail or needs to be further investigated - in terms of meeting the requirements. If a concept fails to meet one of the requirements it is eliminated and does not carry forward to the next step. However, if the concept fulfills or needs to be further investigated it continues forward to the next phase to be further tested and evaluated.

3.6 Experimentation

To later evaluate the feasibility of the considered concepts, experiments were conducted to collect data on their performance. The experiments consisted of pressure testing, where the air-tightness of the cabs was tested to check the pressures that can be achieved, and whether or not different pressure-based methods can be used for detection of leaks. The second part of experimentation aimed to evaluate different localization methods, which also are dependent on pressurizing the cab. The result

from performed experiments was then used in order to aid and serve as evidence in the justification of the decisions regarding concepts and the final recommendation.

Furthermore, the experiments were carried out on standard spec FH or FM cabs produced on the cabtrim production line. To guarantee reliable testing it was ensured that the cabs chosen had been approved in all of the production lines quality control zones, and were ready for either marriage with the chassis, or shipping to Knock Down (KD) factories abroad.

3.6.1 Pressure Testing

This section describes the experimental setup utilized for data collection during pressure experiments.

3.6.1.1 Hypothesis

The objective of this experiment is twofold, firstly to evaluate the air-tightness of vehicle cabins by measuring how high of a stable pressure can be achieved, and further understand the pressure decay, alternatively retention, under controlled airflow and temperature conditions. Secondly, the experiment aims to identify if there is measurable pressure differentiation between a watertight and non-watertight cabs. In line with these objectives, the experiment aims to evaluate the following hypothesis:

1. Air tightness - Pressure Generation

- H_0 (Null): The cab is airtight enough so that high pressure differentials can be achieved in comparison to atmospheric pressure.
- H_1 (Alternative): The cab leaks so much air that no internal overpressure can be achieved.

2. Pressure Decay

- H_0 (Null): The drop in pressure is steady and measurable once the airflow is stopped.
- H_1 (Alternative): The pressure drop is too quick (instantaneous) and cannot be measured.

3.6.1.2 Variables

During the experimentation, several variables were considered and evaluated according to their role within the experiment, these are summarized in *Table 3.1*. Controlled variables included fixed conditions such as cabin doors and luggage compartments being fully closed, and sealed escape vents together with stable ambient conditions. Two independent variables were manipulated: the airflow rate, specified as a percentage setting, and the cab internal temperature. The dependent variables measured in response to these conditions were the internal cab pressure and the pressure decay over time, which served as key indicators of system behavior during testing.

Table 3.1: Variables during pressure experimentation.

Type	Variables
Controlled	Cabin doors & Luggage compartment - Fully Closed
	Front Lid - Open
	Windows - Closed (Exception for air inlet)
	Escape Vents - Sealed
	Fan Position - Fixed
	Ambient Conditions
Independent	Airflow Rate - given as percentage setting
	Water-tightness (Screw under front lid)
	Cab Internal Temperature
Dependent	Internal Cab Pressure
	Pressure Decay Time

3.6.1.3 Experimental Setup & Equipment

The experimentation requires the following equipment to be carried out and data collection. The setup is show in *Figure 3.3*.



Figure 3.3: Main test setup used for pressurization and experimentation.

1. Test Equipment

- A fan with the possibility to adjust power-level and temperature, an EL-Björn TF 18EL EBC was used for this.
- Power cable with pin connectors used to connect power to the cab.
- Adapter module for connecting and directing the airflow from the fan into the cab, a rendering can be seen in *Figure 3.4*.
- Tape for sealing the cabs escape-vents, and other holes.

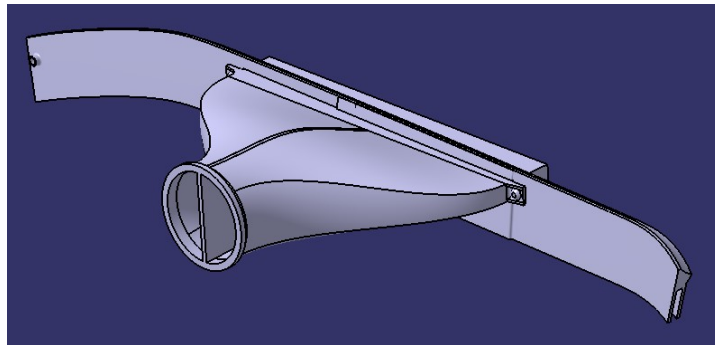


Figure 3.4: CAD render of adapter module used for pressurization. Further and additional specifications of the adapter can be seen in the 2D drawing found in *Appendix A.1*.

2. Measurement Instruments

- Digital Micro-manometer for pressure measurements in the cab, and air-flow measurements.
- Thermometer for temperature measures inside the cab.
- Stopwatch for measuring time-intervals for sampling.

3.6.1.4 Procedure - Pressure Testing

The procedure below presents the steps followed during the pressure testing.

1. Preparation and baseline measurements

- (a) Connect power to the cabin and attach the fan module to the left-hand side window.
- (b) Seal escape vents in the luggage compartments, and the screw holes in the wheel wells.
- (c) Ensure and verify that all windows, doors and luggage compartments are closed.
- (d) Measure baseline ambient pressure and temperature.
- (e) Measure baseline internal pressure and temperature.

2. Fan activation

- (a) Set desired airflow and temperature.
- (b) Begin pressurizing cabin until a stable pressure is achieved, wait for 30s and then log the average pressure.

3. Pressure Decay

- (a) Stop the fan.
- (b) Observe pressure decay over time, measure the pressure data every 30s for a total period of 5min.

4. Repetition

- (a) Test across all planned airflow and temperature levels, where two runs are done per setting, for consistency, and log the run data in accordance with the table in *Appendix A.2*.

3.6.2 Leak Identification

These experiments aimed at seeing how different common leak points behave under a state of overpressure, with constant air flow and temperature and if the pressure drop can be used to clearly identify the presence of a leak.

3.6.2.1 Hypothesis

- H_0 (Null): No significant pressure drop can be observed when a leak point is introduced into the cab.
- H_1 (Alternative): The pressure drop caused by common leaks is clear and significant to indicate the presence of a leak.

3.6.2.2 Variables

During the leak identification experimentation several variables were considered and evaluated according to their role within the experiment, as summarized in *Table 3.2*. In this setup, airflow rate and internal cab temperature were also maintained as controlled variables rather than being varied. The independent variable manipulated was the leak location, while the internal cab pressure was measured as the dependent variable to assess system response.

3.6.2.3 Equipment and Measurement Instruments

For the leak identification experiment the equipment and measurement instruments remained the same as the previous experiment, hence it can be found in *3.6.1.3*.

Table 3.2: Variables during pressure experimentation.

Type	Variables
Controlled	Cabin doors & Luggage compartment - Fully Closed
	Front Lid - Open
	Windows - Closed (Exception for air inlet)
	Escape Vents - Sealed
	Fan Position - Fixed
	Ambient Conditions
	Airflow Rate - given as percentage setting
	Cab Internal Temperature
Independent	Leak Location
Dependent	Internal Cab Pressure

3.6.2.4 Procedure

1. Setting base value - watertight state

- (a) Pressurize the cab to a stable pressure and temperature, slightly over room temperature to achieve a higher pressure.
- (b) Once the pressure is stable start the stopwatch for 30s and record the average pressure.

2. Recording leaking state

- (a) Remove the item that would result in a leak, according to *Appendix A.3*.
- (b) Once the pressure is stable, start the watch for 30s and record the average value.

3. Data collection and repetition

- (a) Record the result, noting the leak position, and average pressure.
- (b) Repeat Procedure for all positions seen in *Appendix A.3*.

3.6.3 Leak Localization - Thermal Imaging

This section describes the experimental setup utilized for data collection during thermal imaging experiments.

3.6.3.1 Hypothesis

The objective of this experiment is to evaluate the possibility to discover and locate leaks in the truck cabin under controlled airflow and temperature conditions using a thermal imaging camera. In line with this objective, the experiment aims to evaluate the following hypothesis:

- H_0 (Null): There is no identifiable differentiation between before and after thermal images, and the differences do not accurately show the simulated leaks.
- H_1 (Alternative): There is a clear identifiable differentiation between before and after thermal images, and the differences accurately show the simulated leaks.

3.6.3.2 Equipment and Measurement Instruments

For the leak identification experiment the equipment and measurement instruments remained the same as the previous experiment, however with the addition of an FLIR IR Camera, the remaining equipment can be found in *3.6.1.3*.

3.6.3.3 Procedure

1. Start up the thermal imaging equipment.
2. Take pictures of the interest points of the cab.
3. Store the pictures.
4. Pressurize the cab to a stable pressure, the same way as done in *3.6.1.4*, steps 1-2.
5. Take pictures of the same points, from the same angle and position, once the cab is pressurized and is up to the desired internal temperature.
6. Store pictures.
7. Compare before and after images.
8. Check for actual leak where indicated by images.
9. Record result.

3.6.4 Leak Localization - Ultrasound

This section describes the experimental setup utilized for data collection during ultrasound experiments.

3.6.4.1 Hypothesis

The objective of this experiment is to evaluate the possibility to discover and locate leaks in the truck cabin under controlled airflow and temperature conditions using

an ultrasonic camera. In line with this object, the experiment aims to evaluate the following hypothesis:

- H_0 (Null): Ultrasound images do not correctly identify leak locations.
- H_1 (Alternative): Ultrasound images correctly show leak locations.

3.6.4.2 Equipment and Measurement Instruments

For the leak identification experiment the equipment and measurement instruments remained the same as the previous experiment, however with the addition of an FLIR Ultrasonic Camera, the remaining equipment can be found in *3.6.1.3*.

3.6.4.3 Procedure

1. Pressurize the cab to a stable pressure, the same way as done in *3.6.1.4*, steps 1-2.
2. Start up the ultrasonic camera.
3. Pressurize the cab using the same procedure as for pressure experimentation until the highest stable pressure it reached.
4. Take pictures of the interest points of the cab.
5. Store pictures.
6. Analyze images for acoustic signals to identify leaks.
7. Check for actual leak according to the image results.
8. Record result.

3.6.5 Concept evaluation

The results from the experiments were evaluated, and discussed with different stakeholders to make a collective decision on how to move forward with each concept. The evaluation process combined both quantitative analysis and qualitative assessment due to difference between the methods.

As previously described, the pressure testing followed a Design of Experiments (DOE) approach. Experimental results were statistically analyzed, with a focus on identifying significant factors affecting pressure behavior. Evaluation criteria included statistical significance, trend analysis and mean pressure values. This allowed for a data-driven understanding of how reliably the method could detect and quantify leaks under controlled environments.

In comparison, thermal imaging was assessed using before-and-after pictures, with simulated leaks introduced to visualize airflow escape points. Since the method is based on graphical interpretation, the evaluation relied heavily on visual inspection of thermal images. The focus was on how clearly the leaks appeared in the images, consistency across different conditions and the thermal patterns and complications.

Ultrasound testing followed a procedure similar to the thermal imaging approach. Simulated leaks were introduced and images of the detected ultrasonic pictures were captured. These were compared against potential environmental disturbances to assess the method's sensitivity and selectivity. Evaluation focused on how clearly leaks could be distinguished and how reliably the system could pinpoint known leak locations.

4

Results

In the following chapter the results of the project are presented. The results follow the chronological order of the methodology, however the results for each section is the summary of the final results including parts that has been iterated more than once.

4.1 Mapping demands and requirements

As mentioned in *Subchapter 3.2*, the requirement specification was divided into two categories, where the first one was the focus of this project. The full requirement specification can be found in *Appendix A.4*. In the full specification, it is also defined if the specifications are actual requirements or desires. The upcoming paragraphs give an initial presentation and short description of requirements, focusing on the first category.

Category one, is *Performance Requirements*, and as the name suggests they describe how the detection method is expected to perform to be considered for further development or deployment. These requirements can be seen in *Table 4.1*. Requirement *1.1* and *1.2* was established and are requirements on the tests ability to detect the presence of a leak. The *Detection Sensitivity* refers to the tests ability to register leaks no matter the size, meanwhile *Detection Accuracy* covers the requirement of correctly verifying leaks or not. In contrast requirements *1.3* and *1.4* focuses on the test ability to localize a leak - an important distinction from detecting a leak. *Localization Sensitivity* addresses the tests capability of being sensitive enough to register and localize a leak no matter size. Conversely, *Localization accuracy* is connected to the ability of correctly locate a leak within a set radius.

Requirement *1.7* is established as a requirement with respect to *Pressure Generation* and covers the ability of generating a sufficient pressure without damaging the structural integrity of the cab. In addition requirement *1.8* and concerns the *Test Medium* and is inherited from the problem description and delimits the project to using compressed air.

The second category in the specification covers overall requirements and desires that need to be considered when developing the concept further, and working on prototypes - these can be seen in *Table 4.2*.

Table 4.1: Performance requirements with respective number extracted from the full specification.

1. Performance Requirements	
1.1	Detection Sensitivity
1.2	Detection Accuracy
1.3	Localization Sensitivity
1.4	Localization Accuracy
1.7	Pressure Generation
1.8	Test Medium

Table 4.2: The remainder of the defined requirements.

Number	Requirement	Number	Requirement
2	Reliability & Durability	7	Operator Requirements
2.1	Maintainability	7.1	Training level
3	Capacity & Scalability	7.2	Ease of use
3.1	Modularity / Upgradability	7.3	Number of operators
3.2	Scalability	7.4	Emitted Noise
4	Process Requirements	7.5	Emitted Vibrations Hand/Arm
4.1	Location	7.6	Emitted Vibrations Whole Body
5	Operating Conditions	8	Equipment Requirements
5.1	Temperature	8.1	Material
5.2	Noise	8.2	Weight
5.3	Vibration	8.3	Ergonomics
6	Level of Automation	8.4	Size
6.1	Automatic Detection	9	Legal & Directives
6.2	Semi-automatic Detection	9.1	Electromagnetic emission
6.3	Manual Detection	9.2	General Health and Safety
6.4	Automatic Localization	9.3	Voltage and Electricity
6.5	Semi-automatic Localization	9.4	Pressure
6.6	Manual Localization		

4.2 Concept Generation and Screening

Once the requirements were defined and information on existing technology was gathered, it was time to start brainstorming solutions and generating concepts. The first step was to map the different functions of the process, which can be seen in *Table 4.3*. Solutions to each function were then brainstormed during multiple sessions, where the requirements and feasibility was kept in mind.

Table 4.3: The different sub-functions and their respective sub-solutions used for in the morphological matrix in order to generate concepts from solution combinations.

Cab Pressurization	Pressure Stabilization	Leak Detection	Leak Localization
Overpressure	Pressure monitoring	Pressure decay	Thermal imaging
Underpressure	Flow monitoring	Flow level	Ultrasound
	Preset time		

The function groups and solutions were then inputted into the program Morpheus to generate all the possible combinations, where impossible pairings were marked to be automatically discarded. The result from this was a morphological matrix that can be seen in *Table 4.4*.

It was then time to start eliminating solutions, in order to have just a few for experimentation. An elimination matrix was used at this stage. The concepts were cross checked against the requirements from the requirement specification, their feasibility, and whether they fulfill the company's directive and then classed as "Y" (Requirement fulfilled), "N" (Requirement not fulfilled), and "?" (More information needed). All concepts with at least one "N" were eliminated, and those left were carried over for experimentation. The elimination matrix can be found in *Appendix A.5*. The remaining concepts can be seen in *Table 4.5*.

4. Results

Table 4.4: The different solutions generated after combining the sub-functions in a morphological matrix.

Solution	Pressurization	Stabilization	Detection	Localization
1	Overpressure	Pressure monitoring	Pressure Decay	Thermal Imaging
2		Flow monitoring		
3		Preset time		
4		Pressure monitoring	Flow Level	
5		Flow monitoring		
6		Preset time		
7		Pressure monitoring	Pressure Decay	Ultrasound
8		Flow monitoring		
9		Preset time		
10		Pressure monitoring	Flow Level	
11		Flow monitoring		
12		Preset time		
13	Underpressure	Pressure monitoring	Pressure Decay	Thermal Imaging
14		Flow monitoring		
15		Preset time		
16		Pressure monitoring	Flow Level	
17		Flow monitoring		
18		Preset time		
19		Pressure monitoring	Pressure Decay	Ultrasound
20		Flow monitoring		
21		Preset time		
22		Pressure monitoring	Flow Level	
23		Flow monitoring		
24		Preset time		

Table 4.5: Final Concepts prior to experimentation.

#	Cab Pressurization	Pressure Stabilization	Leak Detection	Leak Localization
1	Overpressure	Pressure monitoring	Pressure decay	Ultrasound
2	Overpressure	Set Time	Pressure decay	Ultrasound
5	Overpressure	Pressure Monitoring	Pressure decay	Thermal Imaging
6	Overpressure	Set Time	Pressure decay	Thermal Imaging

4.3 Experimentation

This section presents the results of the different conducted experiments. Graphs of pressure behavior, and images from thermal and acoustic imaging are shown and described.

4.3.1 Pressure Testing

In this section the result for the different conducted pressure testing experiments are presented.

4.3.1.1 Pressure Decay

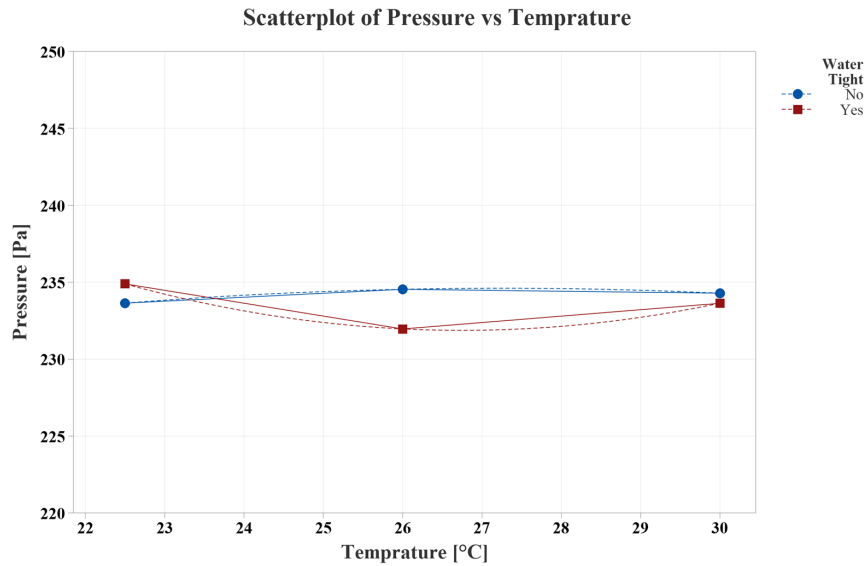
Tests were performed on FH and FM cabs to see how they differ from each other. The first thing that was noticed was how it was possible to achieve almost double the pressure in an FH cab compared to FM, about $650\text{--}700\text{Pa}$ compared to $300\text{--}340\text{Pa}$. This can be due to a number of factors such as the power of the HVAC fan, and the physical properties of the cab. Both cabs had a significant amount of air coming out of different crevices and channels through the sheet metal and various paths. This resulted in the pressure dropping instantly as soon as the inflow of air was stopped, making it impossible to record any measurable pressure decay. For instance, the pressure dropped from the aforementioned stable pressure of each cab to atmospheric pressure in 1-2 seconds, just barely matching the fan powering down. This rapid drop it exceeded the capabilities of the test equipment, making it impossible to measure, deeming the method infeasible.

4.3.1.2 Leak Differentiation Test

The first results from the leak differentiation test were analyzed using the average pressure for two separate runs, different temperatures, different power levels, and a water tight and a non-water tight cab, the raw data from this can be found in *Appendix A.6*. By using average values instead of exact values the idea was that when evaluating a trend it helps to smooth out random fluctuations and noise, making the overall direction of the data clearer.

In *Figure 4.1* the results for a power setting of 50% (of 18kW) is shown. From the results it can be seen that the pressure over different temperatures remained rather steady and the influence of both temperature, and water-tightness yielded a variation within the interval of 232Pa and 235Pa , which may very well be because of random variation within the experiment. An argument that strengthens this claim is the fact that the measures for simulated leaks, meaning a non watertight cab, show a higher pressure reading than for a known watertight cab at the temperatures 26°C and 30°C .

In contrast, the 75% power setting resulted in a clearer distinction between both a water tight and a non-water tight cab, and the temperature's influence starts to become more obvious, as seen in *Figure 4.2*. The results here shows a distinction



Results for Power Level [%] = 50.

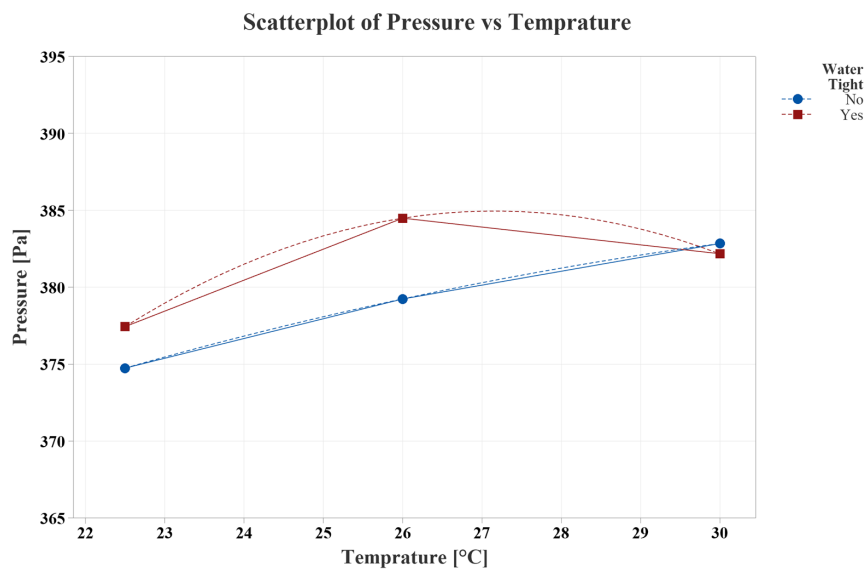
Figure 4.1: Scatterplot showing average pressure levels for watertight and non-watertight cab at different temperatures of the injected air for the power level 50%.

between whether the cab is water tight or not for the two lower temperatures, meanwhile there is an intersection for the higher temperature where the non-water tight cab gave a higher pressure reading. As previously mentioned, a trend can be identified as the average pressure, overall, increased as the temperature rose. However, it is worth noting that the pressure readings still are within a rather small interval, and the largest pressure differential is approximately the relative decrease of 1.4% between an watertight and non-watertight cab at 26°C.

As the power level setting is further increased to the maximum of 100% the effect of increasing temperature was clear, as seen in *Figure 4.3*. However, its noticeable that the influence seems to be more significant in the interval from 22.5°C to 26°C, than from 26°C to 30°C. Besides this, there is a distinction between the water tight and non-watertight cab in terms of pressure for the lower temperature, with an increase in the size of the pressure drop, however the relative pressure differential does decrease to approximately 0.7% which is an halving from the same measure for a power level of 75%.

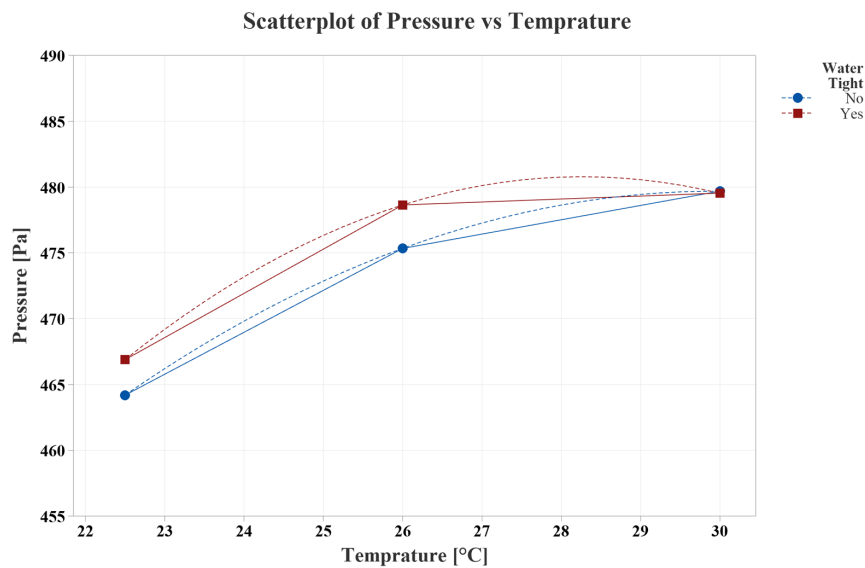
If the plots for the power settings of 75% and 100%, *Figure 4.2* and *4.3* respectively, are further compared it can be seen that there is a clearer distinction between the water tight and non-water tight states in terms of pressure levels at the two lower temperatures suggesting that there might be a more significant interaction happening under these circumstances.

To further understand how the pressure differentiated between runs and different conditions the individual measurements were plotted, these can be seen in *Figures 4.4-4.6*. By doing this its easier to evaluate the individual behavior and trends that otherwise could be missed.



Results for Power Level [%] = 75.

Figure 4.2: Scatterplot showing average pressure levels for watertight and non-watertight cab at different temperatures of the injected air for the power level 75%.

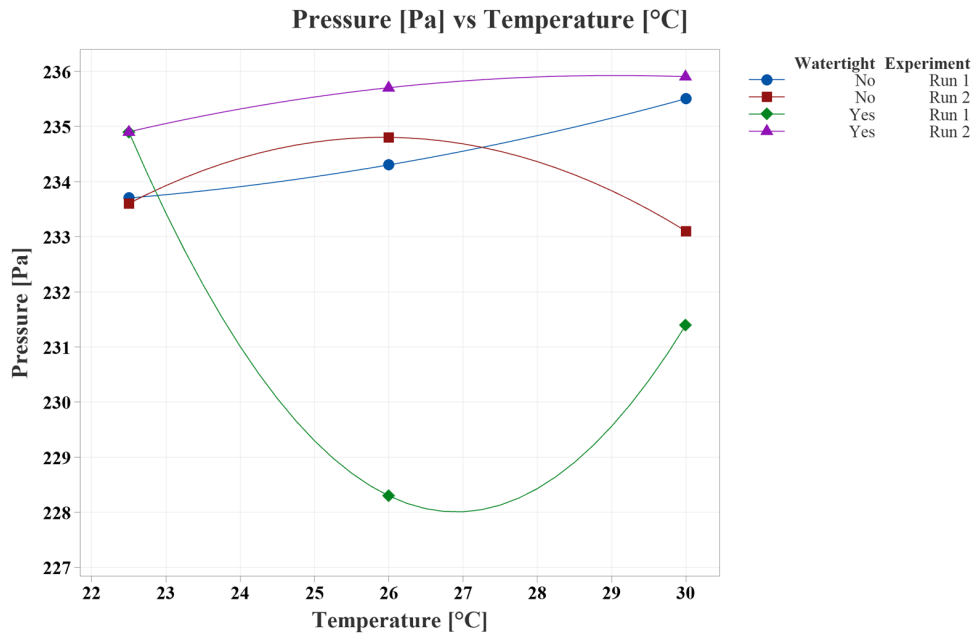


Results for Power Level [%] = 100.

Figure 4.3: Scatterplot showing average pressure levels for watertight and non-watertight cab at different temperatures of the injected air for the power level 100%.

4. Results

By comparing the figures one main takeaway is that as the power level increases the measurements stabilize and converge to a clearer trend as the spread between different points decreases. However, the reason for this remains unknown but one reason could be that the fan used for the experiment operates at a steadier state as the power is increased. An alternative is that the increased power level, which results in increased pressure, makes the pressure readings less sensitive to ambient disturbances as they become relatively smaller as the pressure is increased.



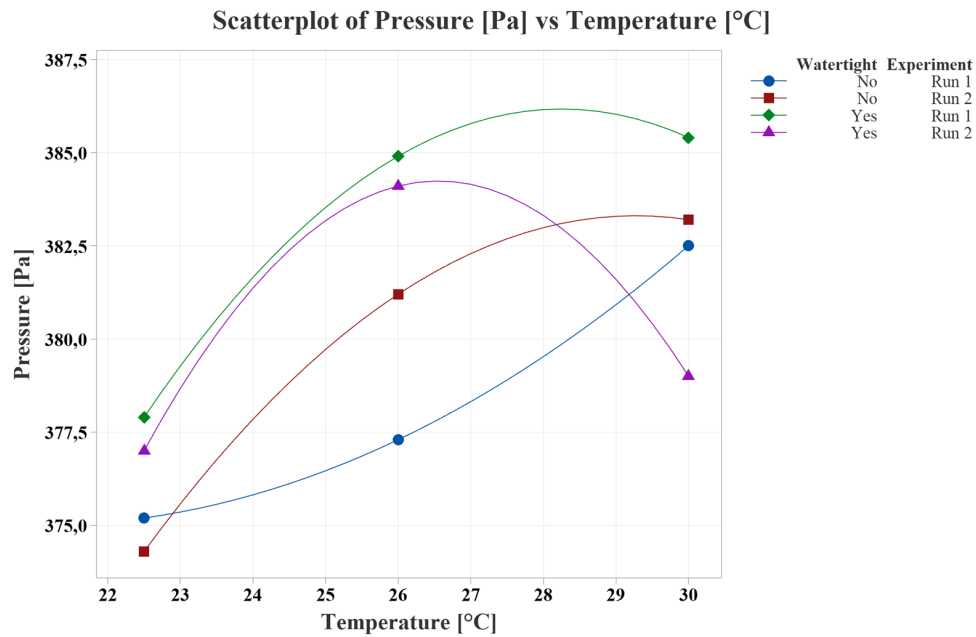
Results include rows where 'Power Level [%]' = 50.

Figure 4.4: Showing the pressure achieved at different temperatures, at power level 50%, for watertight and non-watertight cabs at two different experimental runs.

Furthermore, in the results presented in the Pareto chart of the standardized effects, in *Figure 4.7*, it is possible to evaluate the influence of the different parameters. The result seen is based on the DOE full factorial design.

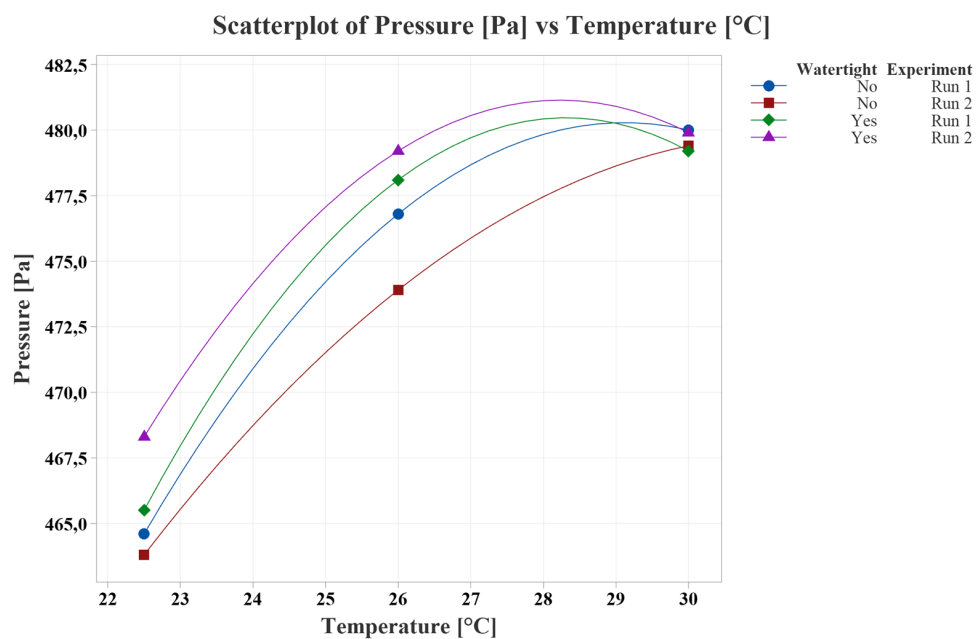
The analysis shows that power level (Factor B) has the most significant influence on the pressure, with a standardized effect well above the significance threshold of 2.10 ($\alpha = 0.05$). Temperature (Factor A) also shows a statistically significant effect, although smaller than that of power level. Furthermore, the interaction between temperature and power level (AB) is significant, indicating that the combined influence of these two factors on pressure is interactive rather than purely additive.

In contrast, the water-tightness factor (C), along with the related interactions (AC, BC, and ABC) did not reach statistical significance. This suggests that under the conditions of this experiment the water tightness did not have a measurable impact on the pressure response. This means that the experiments goal of assessing whether water tightness would result in a detectable drop in pressure tells us that this is not the case - a leak cannot with statistical significance be detected based on the pressure drop.



Results include rows where 'Power Level [%]' = 75.

Figure 4.5: Showing the pressure achieved at different temperatures, at power level 75%, for watertight and non-watertight cabs at two different experimental runs.



Results include rows where 'Power Level [%]' = 100.

Figure 4.6: Showing the pressure achieved at different temperatures, at power level 100%, for watertight and non-watertight cabs at two different experimental runs.

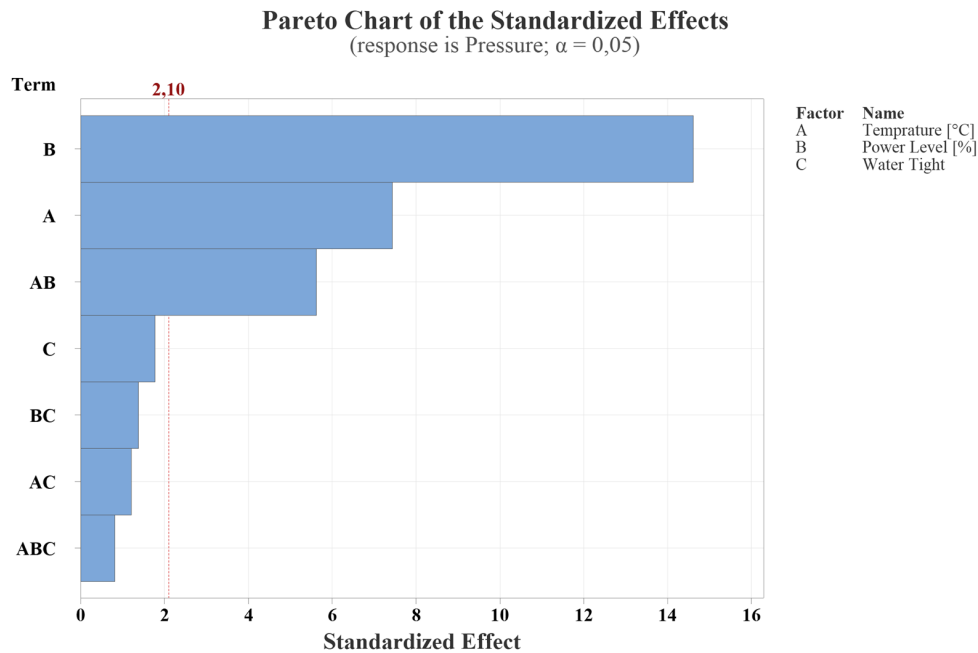


Figure 4.7: Pareto chart showing the standardized effect for the given significance level of 0.95.

However its important to reflect on the result, and the absence of significance in this case may indicate a limitation in the test execution rather than confirming that water tightness is irrelevant and does not affect the pressure. As such, while water tightness appears non-significant in this dataset, a more functioning and reliable test setup could demonstrate a statistically significant effect from this factor.

In addition, how the different factors effected the mean pressure can be seen in *Figure 4.8*. It here becomes even more obvious how the different factors do effect the result. It is here possible to conclude that the power level has a significant larger impact, however this could also effect how the regression captures the significance of the water tightness factor since the size of a possible influence gets greatly out trumped by the power levels influence. The full result from the DOE including residuals can be seen in *Appendix A.7*.

The results from the now 2-level factorial design can be seen in *Figure 4.9*, whereas the entire regression-result can be found in *Appendix A.8*. The same dataset was used for the analysis, with temperature, power level, and water tightness as the independent factors, and internal pressure as the response variable. From the results, power level (B) continues to have a highly significant and dominant effect on pressure with a standardized effect far above the critical value. This confirms that power input is the primary driver of pressure buildup in the system. Temperature (A) also shows a smaller but measurable effect, although not near the same magnitude as the power level.

In contrast to the previous analysis, water-tightness (C) is now seen as a statistically significant factor. This indicates that factor does influence the pressure response un-

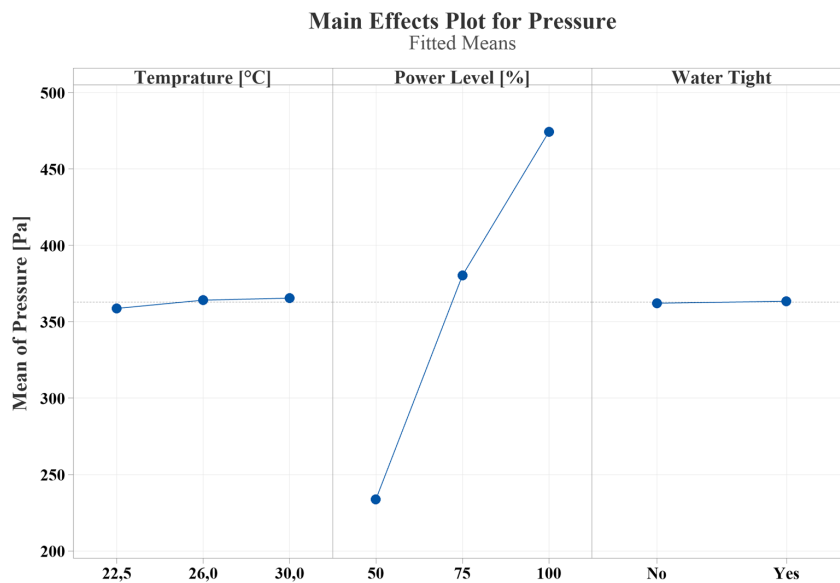


Figure 4.8: Main effect plot showing the mean of pressure given changes in temperature, power level and water tightness.

der these refined test conditions. The ability to detect the effect of water tightness here suggests that lower temperature and higher power level are more ideal conditions to perform the test at.

This result supports the notion that a water tightness plays a meaningful role in maintaining internal pressure. However, as also seen in main effect plot in *Figure 4.10* the power level continues to greatly trump both water tightness and temperature in its influence on the pressure, leaving the margin for error in readings large in comparison to the water tightness factors influence. In addition an change in the set level of significance could also result in the water tightness factor losing its influence, something that ideally should be further investigated and analyzed in terms of potential method implementation and performance requirements.

4. Results

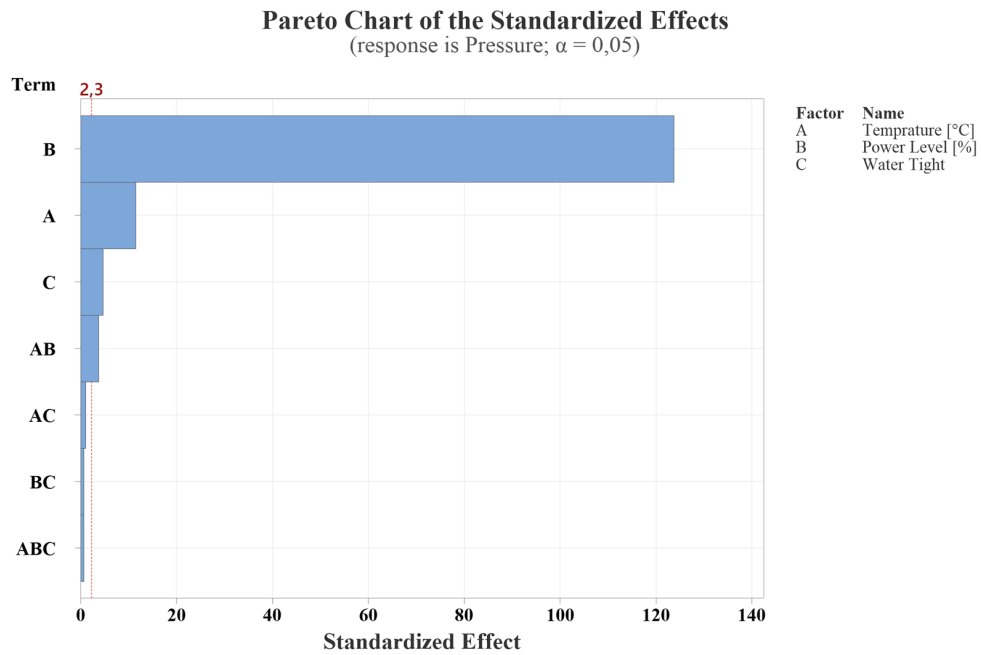


Figure 4.9: Pareto chart showing the standardized effect for the given significance level of 0.95 when only evaluating the two lower temperatures, and two highest power levels.

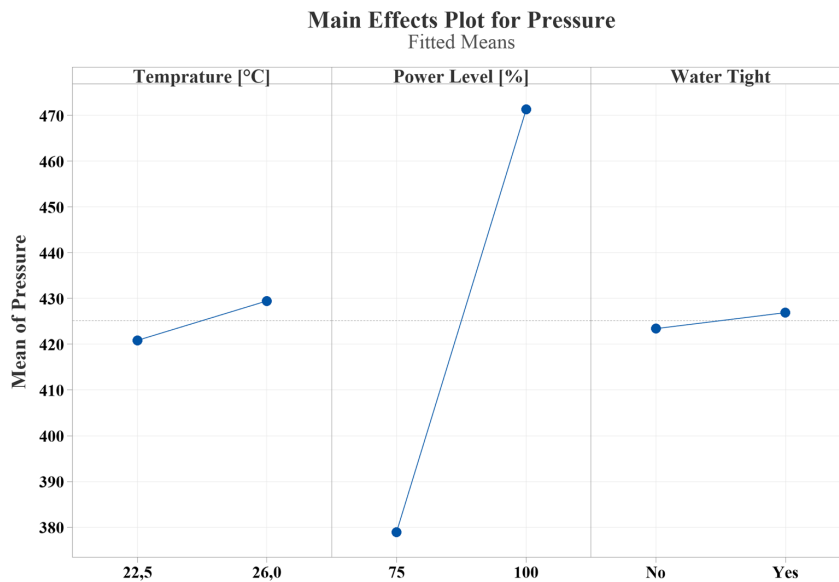


Figure 4.10: Main effect plot showing the mean of pressure given changes in temperature, power level and water tightness for two levels of temperature and power level.

4.3.2 Leak Identification

The leak identification experiments resulted in pressure delta numbers for the different types of leaks, which can be seen in *Figure 4.11*. The results showed that the pressure drop caused by leaks is quite insignificant as it barely falls short of the error margin considered for the experiments. It can also be observed that leaks from different locations result in similar drops in pressure, with some insignificant variation, making it difficult to differentiate between them.

In addition, one important finding was that the maximum pressure for the cabs varied greatly. Even if the same specified cab model was tested the pressure readings varied too much making it impossible to establish a baseline maximum pressure, which then would have been compared again to determine if the cab is tight or not. The underlying reason for this is believed to be overall variation in the manufacturing process. However, this is also further influenced by all the different cab variants produced. In conclusion this means that these results show that this method is unreliable for the current application.

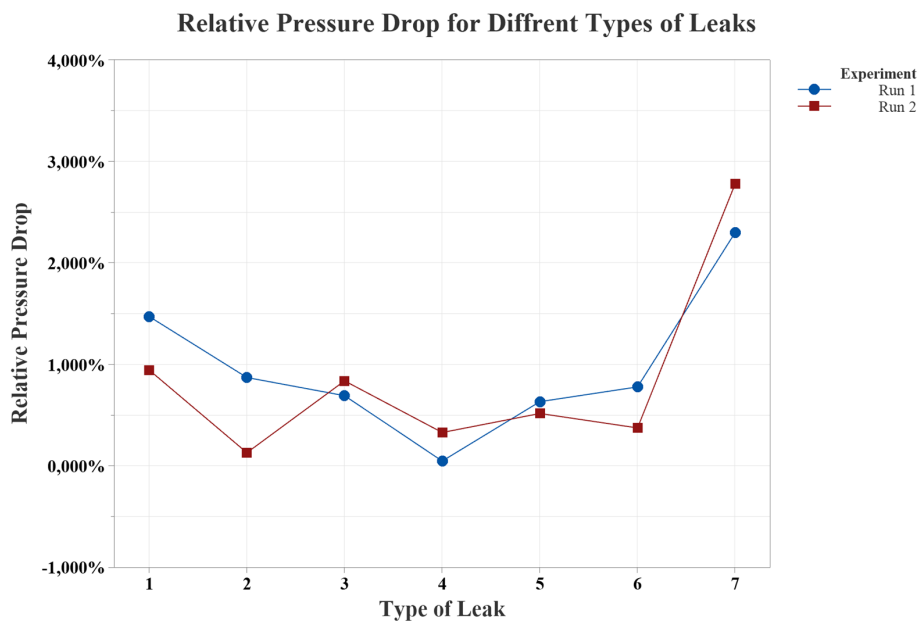


Figure 4.11: Showing the relative pressure loss of different leak points in comparison to maximum pressure, achieved before the leak was created, for two different experimental runs.

4.3.3 Leak Localization

This section presents the results from the leak localization experimentation.

4.3.3.1 Thermal Imaging

The results from thermal imaging experiments were in form thermal images pictures of the points of interest before- and after-pressurization and heating, as described

in 3.6.3.3. The differences between the thermal images were checked to see if the images show the presence of a leak. The chosen points of interest were those most likely to be picked up by the camera, mainly spots with possible leak points close to the surface and little isolation, such as grommets, screws, or badly fit sealings. The presence of insulation in different forms hindered the propagation of heat to the outer shell which largely affected the results in the images. Each image shows the temperature of the point at which the crosshair is pointed, but that shows no information as the angles and distances differ slightly. The images also show the temperature scale in the form of a gradient as well as the automatically set min and max temperatures as per the image. Image 1 in *Table 4.6* shows the entire cab, and it can be clearly seen that there is no noticeable differences before and after pressurization and heating. The image is also affected by other heat sources from the room which affect the result. The rest of the images show similar results, where the difference between the before and after pictures is indistinguishable. The image in *Figure 4.12* show how the images are affected by surrounding objects and how that affects the temperature gradient and how visible results are.

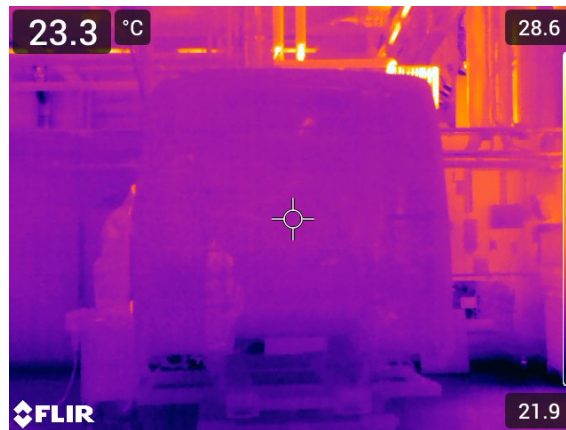
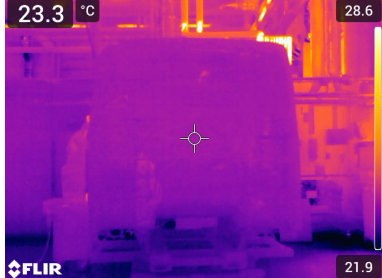
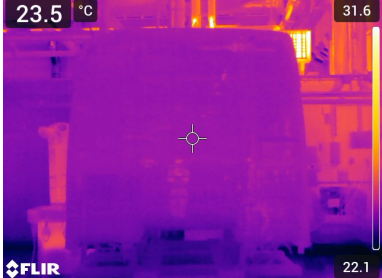



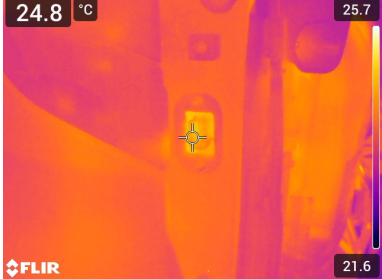
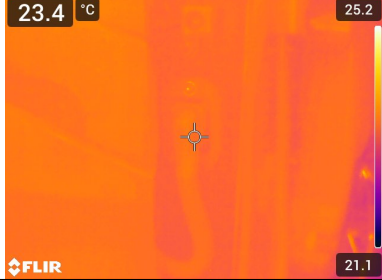
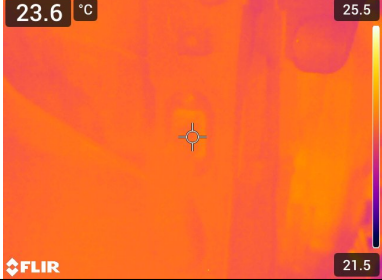




Figure 4.12: Thermal image showing the ambient disturbances when taking a picture at a wider angle.

Another issue noticed was the reflectivity of objects/people off surfaces, which can be seen clearly in image 5 in *Table 4.6*. Finally there was also an issue with transmitted heat from touching anything on the cab, for example when unplugging a contact or opening a door as these were captured by the cameras and the heat was clear in the images which could affect results.

Table 4.6: Thermal Images from various points of interest before and after temperature delta.

#	Description	Before	After
1	Whole cab from behind		
2	Under front-lid area left side CCP plate		
3	Door Contact Right Side Unplugged		
4	Door Contact Right Side Plugged		
5	Door Luggage Compartment		

4.3.3.2 Ultrasonic Imaging



Ultrasonic imaging showed mixed results, where it successfully identified certain leaks, but not others, as well as gave false positives and showed a number of weak-





4. Results

nesses. Leaks that are similar in nature as air leaks were easily captured by the acoustic camera, with accurate positioning. However, there were certain air leaks due to the design of the product that do not cause a water leak which were also captured by the camera. These are false positives, which is a major drawback of this method. Another drawback with the acoustic cameras that was noticed is its sensitivity to ambient sounds, and reflections of sound waves off the cab and the floor.




The best results were when the camera was pointed directly at the point of interest at an angle where no ambient noise is affecting it. This means that the process would be time consuming to check every point individually and double check the result to check for false positives. *Table 4.7* shows pictures of the tested areas. Images 1, 4, 5 show true detected leaks whereas images 2, 3, 6, 7 show false positives. Image 7 shows an area where air gushes out through canals in the Body In White (BIW) which was picked up by the camera and falsely flagged as a leak. Finally, images 8 and 9 show how the images can be vastly affected by ambient noises. Image 8 shows sound reflections off the floor, and image 9 shows noise from forklifts and other sources in production off the cab.

Table 4.7: Ultrasonic Images from various points of interest.

#	Description	Acoustic Image
1	Antenna	
2	Door Contact Connector Left Side	

#	Description	Acoustic Image
3	Door Contact Connector Right Side & Electric connection panel	
4	Intake Grommet & Stud	
5	Intake Grommet & Stud	
6	Area under front-lid	

4. Results

#	Description	Acoustic Image
7	Underside Cab Connector Panel	
8	Backside	
9	Cab on-line	

5

Discussion

This chapter interprets the experimental findings in light of the project goals and production constraints. It evaluates the feasibility of the tested methods, highlights limitations, and offers recommendations for future development.

5.1 Mapping Demands and Requirements

The structured requirements mapping proved valuable in evaluating test concepts. By distinguishing between performance-specific and process-specific criteria, the evaluation gained clarity. However, the ambitious nature of the requirements, particularly those relating to detection accuracy and localization sensitivity, posed challenges for fulfillment with the current setup. A project with a more long-term approach would have had more opportunity to evaluate all requirements, instead of focusing on the performance specific ones.

5.2 Concept Development and Screening

The concept development process successfully generated a range of feasible alternatives through a morphological matrix. However, many theoretically viable configurations were found impractical under real-world conditions, once all constraints were taken into account. For example, flow monitoring-based setups could not be validated experimentally, highlighting a disconnect between theoretical promise and practical applicability.

5.3 Pressure Decay

The pressure decay approach, used to assess cabin air-tightness, was rendered infeasible. Although pressures up to 700 Pa could be reached in FH cabs, the pressure dropped to ambient within 1–2 seconds after airflow was stopped. This rapid decay exceeded the sampling capacity of the measurement equipment and made meaningful analysis impossible. Factors contributing to this include the inherently leaky nature of cab structures and inconsistent sealing using tape. These results suggest that without advanced sealing and equipment upgrades, pressure decay is unsuitable as a leak detection method in this context. However, if future variants of the

produced cabs becomes more air tight this method could be revisited and further evaluated.

5.4 Leak Differentiation Testing

The leak differentiation tests compared internal pressure across watertight and non-watertight cabs under varying airflow conditions. Despite some observable differences, significant pressure overlap was recorded, especially at higher temperatures and power levels. In certain instances, watertight cabs even produced lower readings than their leaking counterparts. This overlap presents a major limitation if the method is intended for binary leak detection.

The cause of this overlap remains uncertain, but is likely due to random variation caused by the testing equipment and environmental fluctuations. For example, sealing fit slightly changing when opening and closing the doors. Additionally, the equipment's limited resolution and inconsistent sealing conditions further hinder reliability.

5.5 Leak Identification Accuracy

Simulated leaks showed only marginal pressure differences, often within error margins. The variation in leak location and geometry introduced inconsistency. These results indicate the need for more controlled, standardized leak simulation and improved airflow regulation to increase test sensitivity and repeatability. In retrospect, the used equipment setup was not optimized for high-precision differential pressure testing. A closed-loop pressurization system with real-time flow feedback and digital leak simulation modules would likely yield more reliable data. The current experiment design, though well-intentioned, lacked the technical precision needed to evaluate leak behavior as expected.

5.6 Thermal Imaging

Thermal imaging revealed limited effectiveness in reliably detecting leak points. While some differences were visible under optimal conditions, the method struggled with environmental sensitivity and image interpretation. Variability in camera angle and ambient reflections introduced inconsistencies, while insulation within the cab structure reduced thermal gradients. To mitigate this, care had to be taken in positioning the camera consistently, at a close and narrow angle, and minimizing external influences. Even then, barely any difference was seen in the image and there were no clear cut indicators locating the leaks. Consequently, thermal imaging alone is not robust enough for the application at hand.

Nevertheless, the FLIR E96 thermal camera used during the experiments was appropriate in terms of resolution but the lack of real-time image comparison tools

or automated anomaly detection, made interpretation subjective and dependent on operator experience.

5.7 Ultrasonic Imaging

Ultrasonic imaging provided the most promising results. The FLIR Si2-Pro acoustic camera successfully visualized certain leaks with good accuracy. However, false positives were observed, primarily due to structural airflow paths and ambient disturbances. Additionally, the system's effectiveness was hindered by suboptimal frequency generation.

Due to the relatively low overpressure ($\sim 0.6 \text{ kPa}$) and large leak geometries, the emitted signals fell within the 5–30 kHz range—outside the optimal filtering range of the ultrasonic camera. Expert consultation indicated that an overpressure of at least 3 kPa and leak openings $\leq 1 \text{ mm}$ are ideal for generating detectable ultrasonic frequencies. The current setup could not meet these conditions, which contributed to mixed signals and more difficult filtration.

Overall, ultrasonic imaging holds promise, particularly for use in controlled quality zones or offline diagnostics, but requires further development in equipment specification and process design to be considered for inline implementation. Applying this method would also require further understanding of leak behavior at different points and a large database to more efficiently automate the detection process and filter out false positives.

5.8 Production Constraints

None of the tested methods met all requirements for inline implementation. Key challenges include the absence of automated detection, inconsistent pressure generation, and equipment unsuited for high-repetition use. The production environment introduces disturbances that compromise repeatability and accuracy. Equipment, mainly the fan, used in this study was also not designed for this application, limiting its practical applicability.

5.9 Method Limitations and Future Improvements

A recurring challenge was the inability to distinguish between harmless airflow and critical water ingress leaks. This distinction is essential to avoid false positives and unnecessary rework. Additionally, pressurizing the cab from the inside alters seal behavior which may affect the way leaks are detected or perceived. Understanding this dynamic is vital to interpreting results accurately.

Another issue is the lack of sufficient data. A broader dataset including standardized watertight and non-watertight cabs would enable better benchmarking and potentially support machine learning models for classification. This again ties back to the short term nature of this project, limiting its overall potential.

5.10 Reflection & Future Research

While none of the current methods are ready for full-scale implementation, this study forms a basis for future improvements. Key recommendations include:

1. **Sensor Enhancement:** Use of more sensitive and fast-responding pressure and flow sensors could enable more precise readings for leak identification.
2. **Machine Learning Integration:** Automated analysis of thermal or ultrasonic imaging could reduce false positives and operator dependency.
3. **Hybrid Approaches:** Combining pressure testing with ultrasonic or thermal localization might yield higher reliability than any method alone.
4. **Cab Design Feedback:** Findings may be used to improve cab component designs to inherently reduce air leakage and simplify detection.

6

Conclusion

The evaluation of air-based methods for leak detection in truck cabs showed mixed results. While stable pressurization of cabs could be achieved, the pressure decay method proved infeasible due to the rapid pressure loss once airflow ceased. Additionally, distinguishing between watertight and non-watertight cabs based solely on internal pressure was unreliable, with minimal differentials and overlapping values observed. Environmental factors and variability in cab construction further limited the method's applicability as a standalone solution.

In terms of localization, thermal imaging showed limited effectiveness. The method was highly sensitive to ambient heat, reflections, and the cab's insulating structure, all of which reduced detection accuracy, if not failure to detect completely. As such, it is not considered robust enough for the purpose investigated. Ultrasonic imaging, on the other hand, produced more promising results. The method was able to identify several leaks with good precision, though it was still affected by false positives due to ambient noise and intentional airflow paths. The low system pressure and relatively large simulated leaks constrained its full potential, but the results indicate that ultrasonic imaging could be a viable solution—especially if further developed with advanced filtering and automation.

Overall, no single method fulfilled all performance and integration criteria for direct on-line implementation. However, ultrasonic imaging demonstrated the greatest potential and, with further refinement, could serve as the basis for a waterless leak detection solution. Future work should focus on understanding ultrasonic imaging performance across various leak types and conditions, supported by a comprehensive data set. This is to be able to distinguish clearly between water leaks and air leaks. This is also key to enabling automated detection through machine learning. Improving cab air-tightness, reducing operator dependency, and refining signal filtering will further support scalability and implementation in a production environment.

Bibliography

- [1] Volvo Truck Corporation, *Volvo Aero Series*, 2025. [Online]. Available: <https://www.volvotrucks.se/sv-se/trucks/the-volvo-aero-range.html>.
- [2] A. Venugopal, “Trucks: market data & analysis”, Statista, Tech. Rep., 2024. [Online]. Available: <https://www-statista-com.eul.proxy.openathens.net/study/175983/trucks-market-data-and-analysis/>.
- [3] Volvo GTO, *Water Test Specifications EMEA-P-069*, (Internal document), 2015.
- [4] Volvo GTT, *Technical Requirement 1579690*, (Internal document), 2019.
- [5] Volvo Group, *Tuve plant*, 2025. [Online]. Available: <https://www.volvogroup.com/en/about-us/organization/our-production-facilities/tuve.html>.
- [6] Volvo GTT, *Technical Requirement Water Tightness Cab 24536658*, (Internal document), 2025.
- [7] *Global Car & Automobile Sales - Market Research Report (2014-2029)*. [Online]. Available: <https://www.ibisworld.com/global/industry/global-car-automobile-sales/1320/>.
- [8] *Don't have a leak: What the watertightness tests for ŠKODA cars entail - Škoda Storyboard*. [Online]. Available: <https://www.skoda-storyboard.com/en/skoda-world/innovation-and-technology/technology/dont-have-a-leak-what-the-watertightness-tests-for-skoda-cars-entail/>.
- [9] *This GM Quality Test Checks For Water Intrusion | GM Authority*. [Online]. Available: <https://gmauthority.com/blog/2019/01/this-gm-quality-test-checks-for-water-intrusion/>.
- [10] K. Paynabar, J. Jionghua (Judy), A. John, and P. Deeds, “Robust Leak Tests for Transmission Systems Using Nonlinear Mixed-Effect Models”, *Journal of Quality Technology*, vol. 44, no. 3, pp. 265–278, Jul. 2012, ISSN: 0022-4065. DOI: 10.1080/00224065.2012.11917899.
- [11] S. Golling, K. Freund, and C. Lammel, “Cost-Effective Quality Assurance for Truck Windscreen Bonding”, *adhäsion KLEBEN & DICHTEN 2008 52:4*, vol. 52, no. 4, pp. 28–30, Apr. 2008, ISSN: 2192-8681. DOI: 10.1007/BF03243809. [Online]. Available: <https://link.springer.com/article/10.1007/BF03243809>.

- [12] S. Chen, P. Li, and L. Wang, “Development on dynamic pressure sensor for long pipeline leak detection”, Chinese, in *Proceedings of the World Congress on Intelligent Control and Automation (WCICA)*, 2008, 9162 – 9167, ISBN: 978-142442114-5. DOI: 10.1109/WCICA.2008.4594380. [Online]. Available: <https://www.scopus.com/inward/record.uri?eid=2-s2.0-52149111387&doi=10.1109%2fWCICA.2008.4594380&partnerID=40&md5=99d5b8b926042ba38ae1fb72704ef8c0>.
- [13] L. G. Harus, M. CAI, K. KAWASHIMA, and T. KAGAWA, “CHARACTERISTICS OF LEAK DETECTION BASED ON DIFFERENTIAL PRESSURE MEASUREMENT”, *Proceedings of the JFPS International Symposium on Fluid Power*, vol. 2005, no. 6, pp. 316–321, 2005, ISSN: 2185-6303. DOI: 10.5739/ISFP.2005.316.
- [14] Y. Shi, J. Chang, Y. Wang, X. Zhao, Q. Zhang, and L. Yang, “Gas Leakage Detection and Pressure Difference Identification by Asymmetric Differential Pressure Method”, *Chinese Journal of Mechanical Engineering*, vol. 35, no. 1, p. 44, 2022, ISSN: 2192-8258. DOI: 10.1186/s10033-022-00697-1.
- [15] P. H. Dunlap, C. C. Daniels, J. L. Wasowski, N. G. Garafolo, N. Penney, and B. M. Steinetz, “Pressure decay testing methodology for quantifying leak rates of full-scale docking system seals”, *45th AIAA/ASME/SAE/ASEE Joint Propulsion Conference and Exhibit*, 2009. DOI: 10.2514/6.2009-5319. [Online]. Available: <https://arc.aiaa.org/doi/10.2514/6.2009-5319>.
- [16] X. Shang, “Development of a hydraulic component leakage detecting system using pressure decay signal”, *Dissertations and Theses @ UNI*, Jan. 2015. [Online]. Available: <https://scholarworks.uni.edu/etd/219>.
- [17] H. Wolf, T. Stauffer, S. C. Y. Chen, *et al.*, “Vacuum decay container/closure integrity testing technology. Part 1. ASTM F2338-09 precision and bias studies”, *PDA Journal of Pharmaceutical Science and Technology*, vol. 63, no. 5, pp. 472 –488, Sep. 2009. [Online]. Available: <https://pubmed.ncbi.nlm.nih.gov/20158052/>.
- [18] H. Wolf, T. Stauffer, S. C. Y. Chen, *et al.*, “Vacuum decay container/closure integrity testing technology. Part 2. Comparison to dye ingress tests”, *PDA Journal of Pharmaceutical Science and Technology*, vol. 63, no. 5, pp. 489 – 498, Sep. 2009. [Online]. Available: <https://pubmed.ncbi.nlm.nih.gov/20158053/>.
- [19] J. Patel, B. Mulhall, H. Wolf, S. Klohr, and D. M. Guazzo, “Vacuum Decay Container Closure Integrity Leak Test Method Development and Validation for a Lyophilized Product-Packaging System”, *PDA Journal of Pharmaceutical Science and Technology*, vol. 65, no. 5, pp. 486–505, Sep. 2011, ISSN: 1079-7440. DOI: 10.5731/pdajpst.2011.00780. [Online]. Available: <http://journal.pda.org/cgi/doi/10.5731/pdajpst.2011.00780>.
- [20] L. G. Harus, C. Youn, N. Nagai, H. Furusawa, and T. Kagawa, “A study on leak detection of a household gas supply system using pressure decay method”, *Proceedings of the SICE Annual Conference*, pp. 2987 –2992, Jan. 2008. DOI: 10.1109/SICE.2008.4655175.

-
- [21] S. DePani and P. Fazio, “Airtightness testing of two- And three-unit buildings with a single fan”, *Journal of Architectural Engineering*, vol. 11, no. 1, pp. 19–24, Mar. 2005, ISSN: 1076-0431. DOI: 10.1061/(ASCE)1076-0431(2005)11:1(19).
- [22] E. L. Hult, M. H. Sherman, and I. Walker, “Blower door techniques for measuring interzonal leakage”, *Thermal Performance of the Exterior Envelopes of Whole Buildings - 12th International Conference*, Clearwater, [Online]. Available: https://web.ornl.gov/sci/buildings/conf-archive/2013%20B12%20papers/090_Hult.pdf.
- [23] A. J. Tiberio and P. Branchi, “A study of air leakage in residential buildings”, *Conference and Exhibition - 2013 International Conference on New Concepts in Smart Cities: Fostering Public and Private Alliances, SmartMILE 2013*, p. 2013, DOI: 10.1109/SmartMILE.2013.6708180.
- [24] D. R. Fritz, A. M. Winer, K. Kozawa, D. Pankratz, and D. Gemmill, “Evaluation of Mechanisms of Exhaust Intrusion into School Buses and Feasible Mitigation Measures”, Jan. 2006. [Online]. Available: <https://ww2.arb.ca.gov/sites/default/files/classic/research/apr/past/03-343.pdf>.
- [25] V. Norrefeldt, A. Lindner, and M. Pschirer, *Customizing the BlowerDoor method for leak detection in the aircraft cargo hold*, 2021. [Online]. Available: <https://www.aivc.org/resource/customizing-blowerdoor-method-leak-detection-aircraft-cargo-hold>.
- [26] J. P. Fine, J. Gray, X. Tian, and M. F. Touchie, “An investigation of alternative methods for determining envelope airtightness from suite-based testing in multi-unit residential buildings”, *Energy and Buildings*, vol. 214, p. 109845, May 2020, ISSN: 03787788. DOI: 10.1016/j.enbuild.2020.109845.
- [27] M. Mahmoodzadeh, V. Gretka, S. Wong, T. Froese, and P. Mukhopadhyaya, “Evaluating patterns of building envelope air leakage with infrared thermography”, *Energies*, vol. 13, no. 14, p. 3545, Jul. 2020, ISSN: 19961073. DOI: 10.3390/en13143545.
- [28] A. Cort, “Fixturing for leak testing”, *Assembly*, no. 13, Dec. 2006. [Online]. Available: <https://www.assemblymag.com/articles/85942-fixturing-for-leak-testing>.
- [29] J. Hoffmann, “Failsafe leak testing”, *Quality*, vol. 46, no. 3, pp. 38–41, Mar. 2007. [Online]. Available: <https://www.qualitymag.com/articles/84893-quality-test-inspection-failsafe-leak-testing>.
- [30] L. Adams, “Trace leaks with hydrogen gas”, *Quality*, vol. 45, no. 4, pp. 28–29, Apr. 2006. [Online]. Available: <https://www.qualitymag.com/articles/84781-quality-innovations-trace-leaks-with-hydrogen-gas>.
- [31] E. U. Hurme and R. Ahvenainen, “A Nondestructive Leak Detection Method for Flexible Food Packages Using Hydrogen as a Tracer Gas”, *Journal of Food Protection*, vol. 61, no. 9, pp. 1165–1169, Sep. 1998, ISSN: 0362-028X. DOI: 10.4315/0362-028X-61.9.1165.

- [32] M. Oishi, *JP2002148137A - Leakage inspection method for heat exchanger - Google Patents*. [Online]. Available: <https://patents.google.com/patent/JP2002148137A/en>.
- [33] J. Huang, H. Zhang, Z. Pan, H. Zheng, and Z. Sun, *CN105203269A - Heat exchange tube and tube plate seal-welding helium leakage-detection device - Google Patents*. [Online]. Available: <https://patents.google.com/patent/CN105203269A/en>.
- [34] G. Li, Z. Lu, X. Xu, H. Li, C. Zhao, and J. Zhang, *CN210603768U - Helium mass spectrometer leak detection device for butt weld of pipe and tube - Google Patents*. [Online]. Available: <https://patents.google.com/patent/CN210603768U/en>.
- [35] C. J. Ghazi and J. S. Marshall, “A CO₂ tracer-gas method for local air leakage detection and characterization”, *Flow Measurement and Instrumentation*, vol. 38, pp. 72–81, Aug. 2014, ISSN: 0955-5986. DOI: 10.1016/J.FLOWMEASINST.2014.05.015.
- [36] J. Nobis, “Testing the gas-tightness of cargo holds in bulk carriers [Überprüfung der gasdichtigkeit von laderäumen auf bulk-carrier]”, *Zentralblatt für Arbeitsmedizin, Arbeitsschutz und Ergonomie*, vol. 60, no. 6, pp. 209–210, Jun. 2010, ISSN: 09442502. DOI: 10.1007/bf03344285.
- [37] J. P. Guillaume, “The leak detection tracer gas [La recherche de fuites au gaz traceur]”, *Eau, l’Industrie, les Nuisances*, no. 355, pp. 83–87, Oct. 2012. [Online]. Available: https://www.researchgate.net/publication/296538146_The_leak_detection_tracer_gas.
- [38] H. Xu, M. Matsubara, and N. Matsubara, “Buried Pipeline Leakage Inspection Technology”, *11th Academic Conference of Geology Resource Management and Sustainable Development 2023*, vol. 3, pp. 1197–1200, Jan. 2023. DOI: 10.52202/073371-0151.
- [39] M. L. Kazakevych, V. M. Kazakevych, and S. Xiangyu, “Tightness testing of aviation systems (Review)”, *Technical Diagnostics and Non-Destructive Testing*, vol. 2022, pp. 30–34, Sep. 2022. DOI: 10.37434/tdnk2022.03.05.
- [40] X. Wu, M. Hu, B. Shang, and R. Huang, “A new method for urban gas leak detection and its application”, *Natural Gas Industry*, vol. 31, no. 9, pp. 98–101, Sep. 2011, ISSN: 10000976. DOI: 10.3787/j.issn.1000-0976.2011.09.020.
- [41] A Alousif and S Alali, “Machinery Fault Detection through Ultrasound Technology”, English, in *SPE Middle East Oil and Gas Show and Conference, MEOS, Proceedings*, vol. 2021-November, Society of Petroleum Engineers (SPE), 2021, ISBN: 978-161399772-7 (ISBN). DOI: 10.2118/204812-MS. [Online]. Available: <https://www.scopus.com/inward/record.uri?eid=2-s2.0-85126908067&doi=10.2118%2f204812-MS&partnerID=40&md5=1a6d7f24e5d4011c8817759373dd6a0c>.

- [42] Y. Lyu, M. Jamil, P. Ma, *et al.*, “An Ultrasonic-Based Detection of Air-Leakage for the Unclosed Components of Aircraft”, *Aerospace*, vol. 8, no. 2, 2021, ISSN: 2226-4310. DOI: 10.3390/aerospace8020055. [Online]. Available: <https://www.mdpi.com/2226-4310/8/2/55>.
- [43] S. D. Holland, R. R. Roberts, D. E. Chimenti, and M. Strei, “Ultrasonic spacecraft leak location using structure borne noise”, *The Journal of the Acoustical Society of America*, vol. 115, no. 5_Supplement, p. 2548, Feb. 2004, ISSN: 0001-4966. DOI: 10.1121/1.4809273.
- [44] M Liang, K Yang, M Feng, K Mu, M Jiao, and L Li, “Acoustic Imaging Method for Gas Leak Detection and Localization Using Virtual Ultrasonic Sensor Array”, English, *Sensors*, vol. 24, no. 5, 2024, ISSN: 14248220 (ISSN). DOI: 10.3390/s24051366. [Online]. Available: <https://www.scopus.com/inward/record.uri?eid=2-s2.0-85187511572&doi=10.3390%2fs24051366&partnerID=40&md5=19deab67b1a8c5e384c88a73740f3a58>.
- [45] A. Rajbanshi, D. Das, V. Udutalapally, and R. Mahapatra, “dLeak: An IoT-Based Gas Leak Detection Framework for Smart Factory”, *SN Computer Science*, vol. 3, no. 4, pp. 1–12, Jul. 2022, ISSN: 26618907. DOI: 10.1007/S42979-022-01181-2/METRICS. [Online]. Available: <https://link.springer.com/article/10.1007/s42979-022-01181-2>.
- [46] A. M. Willemsen, F. Poradek, and M. D. Rao, “Reduction of noise in an excavator cabin using order tracking and ultrasonic leak detection”, *Noise Control Engineering Journal*, vol. 57, no. 5, pp. 400–412, Sep. 2009, ISSN: 07362501. DOI: 10.3397/1.3207865.
- [47] W. C. Wilson, N. C. Coffey, and E. I. Madaras, “Leak Detection and Location Technology Assessment for Aerospace Applications”, 2008. [Online]. Available: <https://ntrs.nasa.gov/api/citations/20080041598/downloads/20080041598.pdf>.
- [48] J. Cao, H. Zou, X. Yu, *et al.*, “Detection of plane sealing leakage by tuning the generated sound characteristics”, *Measurement*, vol. 146, pp. 815–826, Nov. 2019, ISSN: 0263-2241. DOI: 10.1016/J.MEASUREMENT.2019.07.029.
- [49] Teledyne FLIR LLC, *Industrial Acoustic Imaging Camera for Partial Discharge Detection, Pressurized Leak Detection and Mechanical Fault Detection - FLIR Si2-Pro*, 2025. [Online]. Available: <https://www.flir.com/products/si2-pro/?vertical=condition%20monitoring&segment=solutions>.
- [50] M. Meister and T. Berlitz, *EP1413869A1 - Method for localizing leaks in vehicles*, 2002. [Online]. Available: <https://patents.google.com/patent/EP1413869A1/en>.
- [51] S. Dudić, I. Ignjatović, D. Šešlija, V. Blagojević, and M. Stojiljković, “Leakage quantification of compressed air using ultrasound and infrared thermography”, *Measurement*, vol. 45, no. 7, pp. 1689–1694, 2012, ISSN: 0263-2241. DOI: <https://doi.org/10.1016/j.measurement.2012.04.019>. [Online]. Available: <https://www.sciencedirect.com/science/article/pii/S0263224112001893>.

- [52] A. Ma, R. Qian, Y. Li, Q. Xie, and S. Dong, “Design of Aeroengine Air Leak Automatic Monitoring System Based on Infrared Thermography”, *Journal of Physics: Conference Series*, vol. 2528, no. 1, p. 12 035, Jul. 2023. DOI: 10 . 1088/1742-6596/2528/1/012035.
- [53] B. Kakillioglu, S. Velipasalar, and T. Rakha, “Autonomous Heat Leakage Detection from Unmanned Aerial Vehicle-Mounted Thermal Cameras”, *Proceedings of the 12th International Conference on Distributed Smart Cameras*, 2018. [Online]. Available: <https://api.semanticscholar.org/CorpusID:52895330>.
- [54] J. Chang, Y. Shi, L. Yang, *et al.*, “Deep Learning Method for Leakage Location Detection of Pneumatic Systems Based on Infrared Thermal Image Evaluation”, in *Proceedings of the 2024 7th International Conference on Software Engineering and Information Management*, ser. ICSIM '24, New York, NY, USA: Association for Computing Machinery, 2024, pp. 77–83, ISBN: 9798400709197. DOI: 10.1145/3647722.3647734.
- [55] O. Attallah, “Multitask Deep Learning-Based Pipeline for Gas Leakage Detection via E-Nose and Thermal Imaging Multimodal Fusion”, *Chemosensors*, vol. 11, no. 7, 2023, ISSN: 2227-9040. DOI: 10.3390/chemosensors11070364. [Online]. Available: <https://www.mdpi.com/2227-9040/11/7/364>.
- [56] Teledyne FLIR LLC, *Advanced Thermal Imaging Camera - FLIR E96*, 2025. [Online]. Available: <https://www.flir.eu/products/e96/?vertical=condition+monitoring&segment=solutions>.
- [57] A. Nowodzinski, O. Ndjoye-Kogou, V. Mourier, *et al.*, “Capacitive micromachined ultrasonic transducers leak detection by dye penetrant test”, *Microelectronics Reliability*, vol. 114, p. 113 908, Nov. 2020, ISSN: 0026-2714. DOI: 10.1016/J.MICROREL.2020.113908.
- [58] INFICON, *Bubble Testing*. Cologne: INFICON, 2016. [Online]. Available: <https://www.bing.com/ck/a?!&&p=ed5393a2098524207f0f6dc125d7302cb89bac63e74572d94f323bd711a60605Jm1tdHM9MTcz0TE0NTYwMA&ptn=3&ver=2&hsh=4&fclid=113b0725-3bb9-6bd4-18c9-12513aec6a52&psq=Bubble+Testing+automotive&u=a1aHR0cHM6Ly93d3cuaW5maWNvbi5jb20vbWVkaWEvNzk5Mi9kb3dubG9hZC8tUG9ydGFscy0wLVBERi11Ym9va3MtSU5GSUNPT19FLUJvb2tftGVha1Rlc3RpbmdJb1RoZUF1dG9tb3RpdmVJbmRlc3RyeV9taWthMDB1bi1iXzE2MDQu cGRmP3Y9MSZsYXRlc3Q9MQ&ntb=1>.
- [59] K. Ueda, “Localization of air leaks by soap bubble”, *Journal of Thoracic Disease*, vol. 11, no. Suppl 9, 2019, ISSN: 2077-6624. [Online]. Available: <https://jtd.amegroups.org/article/view/27572>.
- [60] S. C. Wheelwright and K. B. Clark, *Revolutionizing Product Development: Quantum Leaps in Speed, Efficiency and Quality*. New York, NY: The Free Press, 1992, pp. 111–132, ISBN: 978-1-4516-7629-7.

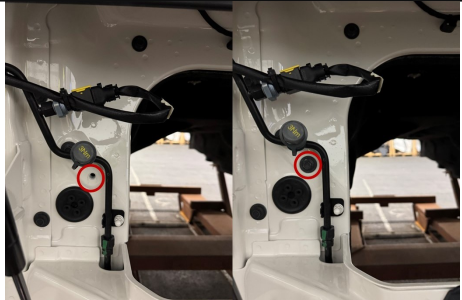


A



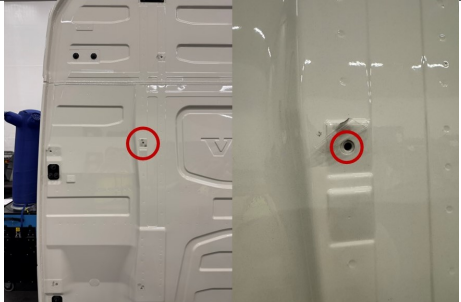
Appendix

A.2 Leak Identification Experiment Template


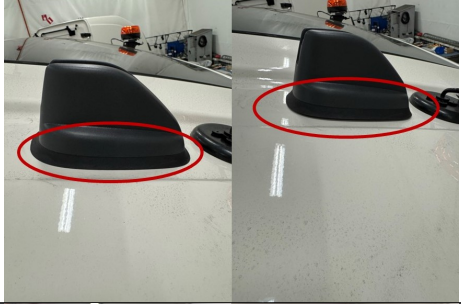

Standard Order	Run Order	Temperature [°C]	Power Level [%]	Watertight	Pressure [Pa]
21	1	22.5	75	No	-
6	2	22.5	100	Yes	-
32	3	30	50	Yes	-
13	4	30	50	No	-
27	5	26	75	No	-
22	6	22.5	75	Yes	-
20	7	22.5	50	Yes	-
35	8	30	100	No	-
7	9	26	50	No	-
12	10	26	100	Yes	-
4	11	22.5	75	Yes	-
29	12	26	100	No	-
11	13	26	100	No	-
24	14	22.5	100	Yes	-
18	15	30	100	Yes	-
10	16	26	75	Yes	-
5	17	22.5	100	No	-
14	18	30	50	Yes	-
31	19	30	50	No	-
19	20	22.5	50	No	-
17	21	30	100	No	-
26	22	26	50	Yes	-
25	23	26	50	No	-
9	24	26	75	No	-
8	25	26	50	Yes	-
34	26	30	75	Yes	-
23	27	22.5	100	No	-
36	28	30	100	Yes	-
15	29	30	75	No	-
1	30	22.5	50	No	-
3	31	22.5	75	No	-
33	32	30	75	No	-
30	33	26	100	Yes	-
28	34	26	75	Yes	-
2	35	22.5	50	Yes	-
16	36	30	75	Yes	-

A.3 Simulated leak locations and causes

#	Location	Leak Cause	Picture
1	Screw under front lid	Missing screw	
2	Door connector contact	Loose screws	
3	Door connector contact	Loose screws, loose contact	

#	Location	Leak Cause	Picture
4	Door connector contact	Loose screws, unplugged contact	
5	Door connector contact	Unplugged contact	
6	Screw hole on backside #1	Missing screw	

A. Appendix

#	Location	Leak Cause	Picture
7	Screw hole on backside #2	Missing screw	
8	Antenna	Loose fit	
9	Beacon light	Loose screws	

A.4 Requirement Specification

Number	Requirement	Description	Target Value	R - Requirement D - Demand	Demand Rating 1-5 (low - high)	Validation Method	Origin
1	Performance Requirements						
1.1	Detection Sensitivity	Ability to detect leaks of different sizes	All sizes, minimum just as well as water-jet test	R		Test	
1.2	Detection Accuracy	Ability to accurately detect the presence of a leak	99% of previous verified defect cabs	R		Test	
1.3	Localization Sensitivity	Ability to locate the location of leaks of different sizes	All sizes, minimum just as well as water-jet test	R		Test	
1.4	Localization Accuracy	Ability to accurately locate leaks	All leak locations within a 0.3m radius of the actual leak	R		Test	
1.5	Test Medium	Medium used to perform the test	Compressed Air	R		Design	
2	Reliability & Durability						
2.1	Maintainability	The ability to maintain and repair the equipment conveniently		R		Equipment Design	Production Maintenance
3	Capacity & Scalability						
3.1	Modularity / Upgradability	Ability to upgrade components and sensors, by having a modular design		D	3	Equipment Design	Production Engineering
3.2	Scalability	Potential to implement solution on a larger scale	Full documentation	R		Process Design	
4	Process Requirements						
4.1	Location	Ability to implement process on line, if functional		D	5	Estimation	
5	Operating Conditions						
5.1	Temperature	Ability to function within a defined temperature range	18-30 °C	R		Equipment Design	EU Health & Safety Directive From (EN 2003/10/CE)
5.1	Noise	Ability to function regardless of the presence of noise (within a given range)	> 80 dB(A) >135 dB(C)	R		Equipment Design	EU Health & Safety Directive From (EN 2003/10/CE)
5.3	Vibration	Ability to resist vibration in the environment	>5 m/s ² .	R		Equipment Design	EU Health & Safety Directive From (EN 2003/10/CE)

A. Appendix

Number	Requirement	Description	Target Value	R - Requirement D - Demand	Demand Rating 1-5 (low - high)	Validation Method	Origin
6	Level of Automation						
6.1	Automatic Detection	System flags detected leaks automatically - instructs operator of the critical area		D	1	Design	
6.2	Semi-automatic Detection	System flags that a leak has been detected - operator manually identifies the critical area		D	4	Design	
6.3	Manual Detection	The operator manually identifies the critical area		R		Design	
6.4	Automatic Localization	The screening/scanning process is automatic and no work is performed by an operator		D	1	Design	
6.5	Semi-automatic Localization	The majority of the screening/scanning is automatic, some areas are complemented by		D	4	Design	
6.6	Manual Localization	The operator manually performs a screening/scan of the cab		R		Design	
7	Operator Requirements						
7.1	Training level	The level of training needed, do operators have to be certified?	~4h	R		Testing	
7.2	Ease of use	How easy is it for a trained operator to perform the tests	Easily achieve high accuracy without needing more training	R		Testing / Survey	
7.3	Number of operators	How many operators are needed to complete the process?	2	R		Testing / Survey	
7.4	Emitted Noise	Emitted noise by the leak test	< 75 dB(A), If the work environment is > 80 dB(A) then < 70 dB(A).	R		Measurement	Volvo GTO Ergonomics and Occupational Guideline From (EN 2003/10/CE)
7.5	Emitted Vibrations Hand/Arm	Emitted vibrations into hands/arms by the leak test	Trigger action at 2.5 m/s ² , exposure limit at 5 m/s ² .	R		Measurement	Volvo GTO Ergonomics and Occupational Guideline From (EN 2003/10/CE)
7.6	Emitted Vibrations Whole Body	Emitted vibrations into whole body by the leak test	Trigger action at 0.5 m/s ² , exposure limit at 1.15 m/s ²	R		Measurement	Volvo GTO Ergonomics and Occupational Guideline From (EN 2003/10/CE)

Number	Requirement	Description	Target Value	R - Requirement D - Demand	Demand Rating 1-5 (low - high)	Validation Method	Origin
8	Production/Integration						
8.1	Takt Time Compliance	Ability to comply to the specified takt time	210 s	R		Test	
8.2	Cycle Time	Ability to comply to the specified cycle time	210 s	R		Test	
8.3	Ergonomics	Follow guideline recommendations		R		Testing / Expert evaluation	Volvo GTO Ergonomics and Occupational Guideline
8.4	Pressure Generation	Ability to generate enough pressure for the simulation without damaging the structure of	Come up to 500 Pa within 30 seconds, stable pressure	R		Test / Equipment Specifications	Product Developer & Quality Engineering
9	Legal and Directives						
9.1	Electromagnetic emission		Certification According to Relevant Directive	R		Measurement / Specifications	EMC Compatibility Directive Directive 2014/30/EU
9.2	General Health and Safety		Certification According to Relevant Directive	R		Measurement / Specifications	Machinery Directive Directive 2006/42/EC
9.3	Voltage and Electricity		Certification According to Relevant Directive	R		Measurement / Specifications	Low Voltage Directive (LVD) Directive 2014/35/EU
9.4	Pressure		Certification According to Relevant Directive	R		Measurement / Specifications	Pressure Equipment Directive Directive 2014/68/EU

A.5 Elimination Matrix

Chalmers		Elimination Matrix for: Waterless water test									
Created by:		Andreas Järlebratt Ibrahim Timraz						Created: 20250304 Modified: 20250315		Page 1	
								- Yes (Y) - No (N) ? More Info Needed		+ Keep Solution - Eliminate Solution	
Solutions	Elimination Criteria (Requirements)								Comment	DECISION	
	Solves main problem	1.1 Detection Sensitivity	1.2 Detection Accuracy	1.3 Localization Sensitivity	1.4 Localization Accuracy	1.5 Test Medium	Feasible (Technically & Economically)	Other (Fulfills company's directive)			
1	Y	?	?	?	?	?	Y	Y		+	
2	Y	?	?	?	?	?	N	Y	Flow level/monitoring not possible to test with current equipment	-	
3	Y	?	?	?	?	?	Y	Y		+	
4	Y	?	?	?	?	?	N	Y	Flow level/monitoring not possible to test with current equipment	-	
5	Y	?	?	?	?	?	N	Y	Flow level/monitoring not possible to test with current equipment	-	
6	Y	?	?	?	?	?	N	Y	Flow level/monitoring not possible to test with current equipment	-	
7	Y	?	?	?	?	?	Y	Y		+	
8	Y	?	?	?	?	?	N	Y	Flow level/monitoring not possible to test with current equipment	-	
9	Y	?	?	?	?	?	Y	Y		+	
10	Y	?	?	?	?	?	N	Y	Flow level/monitoring not possible to test with current equipment	-	

Chalmers		Elimination Matrix for: Waterless water test								
Created by:		Andreas Järlebratt Ibrahim Timraz					Created: 20250304 Modified: 20250315		Page 1	
							- Yes (Y) - No (N) ? More Info Needed		+ Keep Solution - Eliminate Solution	
Solutions	Elimination Criteria (Requirements)								Comment	DECISION
	Solves main problem	1.1 Detection Sensitivity	1.2 Detection Accuracy	1.3 Localization Sensitivity	1.4 Localization Accuracy	1.5 Test Medium	Feasible (Technically & Economically)	Other (Fulfills company's directive)		
11	Y	?	?	?	?	?	N	Y	Flow level/monitoring not possible to test with current equipment	-
12	Y	?	?	?	?	?	N	Y	Flow level/monitoring not possible to test with current equipment	-
13	N	?	?	?	?	?	N	N	Underpressure solutions deemed not feasible as they do not simulate the desired conditions. Therefore all eliminated	-
14	N	?	?	?	?	?	N	N		-
15	N	?	?	?	?	?	N	N		-
16	N	?	?	?	?	?	N	N		-
17	N	?	?	?	?	?	N	N		-
18	N	?	?	?	?	?	N	N		-
19	N	?	?	?	?	?	N	N		-
20	N	?	?	?	?	?	N	N		-
21	N	?	?	?	?	?	N	N		-
22	N	?	?	?	?	?	N	N		-
23	N	?	?	?	?	?	N	N		-
24	N	?	?	?	?	?	N	N	-	

A.6 Leak Identification Experiment Result

Standard Order	Run Order	Temperature [°C]	Power Level [%]	Watertight	Pressure [Pa]
21	1	22.5	75	No	374.3
6	2	22.5	100	Yes	465.5
32	3	30	50	Yes	235.9
13	4	30	50	No	235.5
27	5	26	75	No	381.2
22	6	22.5	75	Yes	377.0
20	7	22.5	50	Yes	234.9
35	8	30	100	No	479.4
7	9	26	50	No	234.3
12	10	26	100	Yes	478.1
4	11	22.5	75	Yes	377.9
29	12	26	100	No	473.9
11	13	26	100	No	476.8
24	14	22.5	100	Yes	468.3
18	15	30	100	Yes	479.2
10	16	26	75	Yes	384.9
5	17	22.5	100	No	464.6
14	18	30	50	Yes	231.4
31	19	30	50	No	233.1
19	20	22.5	50	No	233.6
17	21	30	100	No	480.0
26	22	26	50	Yes	235.7
25	23	26	50	No	234.8
9	24	26	75	No	377.3
8	25	26	50	Yes	228.3
34	26	30	75	Yes	379.0
23	27	22.5	100	No	463.8
36	28	30	100	Yes	479.9
15	29	30	75	No	382.5
1	30	22.5	50	No	233.7
3	31	22.5	75	No	375.2
33	32	30	75	No	383.2
30	33	26	100	Yes	479.2
28	34	26	75	Yes	384.1
2	35	22.5	50	Yes	234.9
16	36	30	75	Yes	385.4

A.7 DOE - Full Factorial Design Result

EXP. 1 - GENERAL FACTORIAL

General Factorial Regression: Pressure versus Temperature [°C]; Power Level [%]; Water Tight

Factor Information

Factor	Levels	Values
Temperature [°C]	3	22,5; 26,0; 30,0
Power Level [%]	3	50; 75; 100
Water Tight	2	No; Yes

Analysis of Variance

Source	DF	Adj SS	Adj MS	F-Value	P-Value
Model	17	352335	20726	4695,54	0,000
Linear	5	352042	70408	15951,56	0,000
Temperature [°C]	2	305	153	34,59	0,000
Power Level [%]	2	351723	175861	39842,73	0,000
Water Tight	1	14	14	3,16	0,092
2-Way Interactions	8	275	34	7,79	0,000
Temperature [°C]*Power Level [%]	4	245	61	13,87	0,000
Temperature [°C]*Water Tight	2	14	7	1,53	0,243
Power Level [%]*Water Tight	2	17	8	1,87	0,183
3-Way Interactions	4	18	5	1,02	0,423
Temperature [°C]*Power Level [%]*Water Tight	4	18	5	1,02	0,423
Error	18	79	4		
Total	35	352415			

Model Summary

S	R-sq	R-sq(adj)	R-sq(pred)
2,10093	99,98%	99,96%	99,91%

Coefficients

Term	Coef	SE Coef	T-Value	P-Value	VIF
Constant	362,689	0,350	1035,80	0,000	
Temperature [°C]					
22,5	-4,047	0,495	-8,17	0,000	1,33
26,0	1,361	0,495	2,75	0,013	1,33
Power Level [%]					
50	-128,847	0,495	-260,20	0,000	1,33
75	17,478	0,495	35,29	0,000	1,33
Water Tight					
No	-0,622	0,350	-1,78	0,092	1,00
Temperature [°C]*Power Level [%]					
22,5 50	4,481	0,700	6,40	0,000	1,78
22,5 75	-0,019	0,700	-0,03	0,978	1,78
26,0 50	-1,928	0,700	-2,75	0,013	1,78
26,0 75	0,347	0,700	0,50	0,626	1,78
Temperature [°C]*Water Tight					
22,5 No	-0,486	0,495	-0,98	0,339	1,33
26,0 No	-0,378	0,495	-0,76	0,455	1,33
Power Level [%]*Water Tight					
50 No	0,947	0,495	1,91	0,072	1,33
75 No	-0,594	0,495	-1,20	0,246	1,33
Temperature [°C]*Power Level [%]*Water Tight					
22,5 50 No	-0,464	0,700	-0,66	0,516	1,78
22,5 75 No	0,353	0,700	0,50	0,621	1,78
26,0 50 No	1,328	0,700	1,90	0,074	1,78
26,0 75 No	-1,031	0,700	-1,47	0,158	1,78

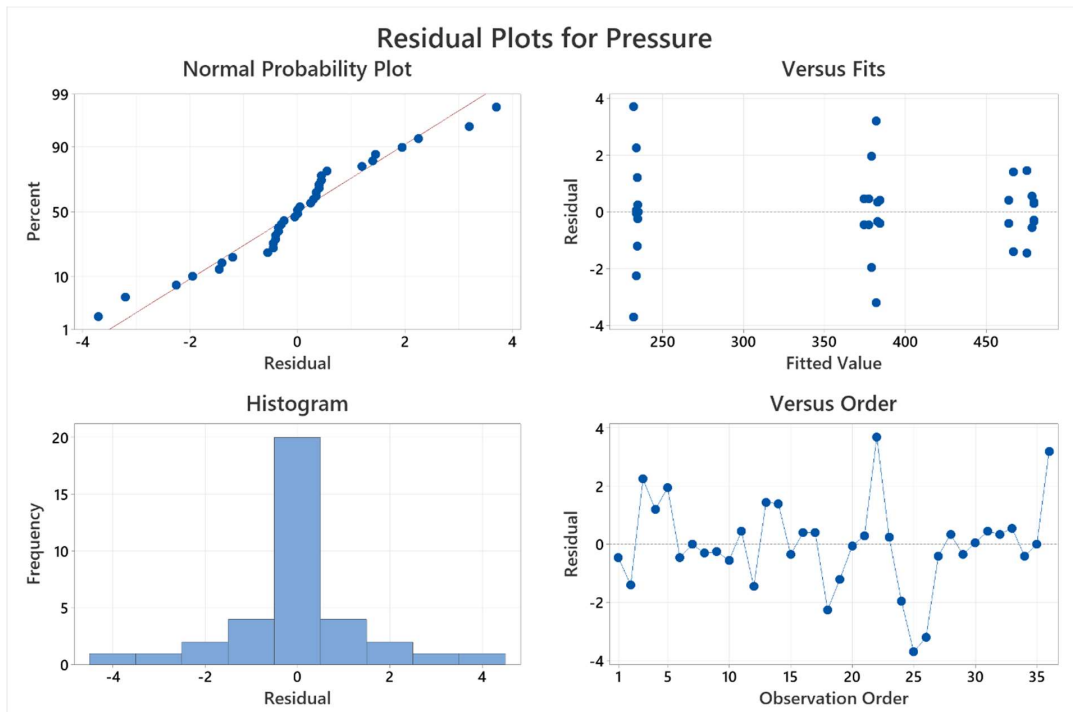
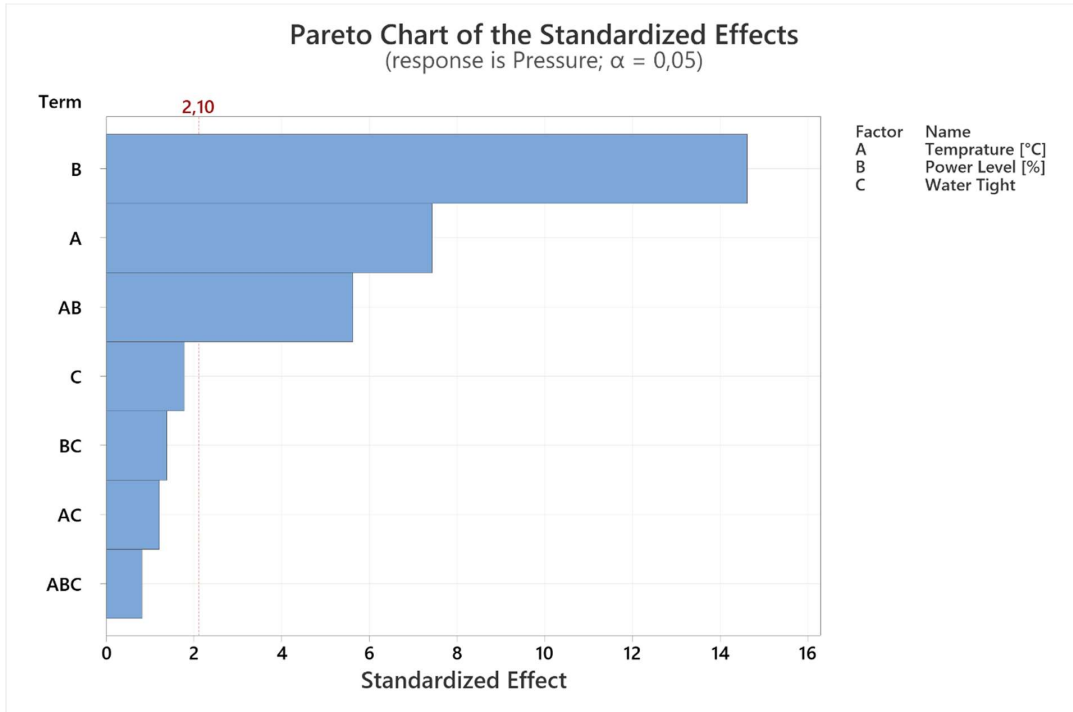
Regression Equation

$$\begin{aligned}
 \text{Pressure} = & 362,689 - 4,047 \text{ Temperature [}^\circ\text{C]}_{22,5} + 1,361 \text{ Temperature [}^\circ\text{C]}_{26,0} \\
 & + 2,686 \text{ Temperature [}^\circ\text{C]}_{30,0} - 128,847 \text{ Power Level [\%]}_{50} \\
 & + 17,478 \text{ Power Level [\%]}_{75} + 111,369 \text{ Power Level [\%]}_{100} \\
 & - 0,622 \text{ Water Tight}_{\text{No}} \\
 & + 0,622 \text{ Water Tight}_{\text{Yes}} + 4,481 \text{ Temperature [}^\circ\text{C]} * \text{Power Level [\%]}_{22,5 50} \\
 & - 0,019 \text{ Temperature [}^\circ\text{C]} * \text{Power Level [\%]}_{22,5 75} \\
 & - 4,461 \text{ Temperature [}^\circ\text{C]} * \text{Power Level [\%]}_{22,5 100} \\
 & - 1,928 \text{ Temperature [}^\circ\text{C]} * \text{Power Level [\%]}_{26,0 50} \\
 & + 0,347 \text{ Temperature [}^\circ\text{C]} * \text{Power Level [\%]}_{26,0 75} \\
 & + 1,581 \text{ Temperature [}^\circ\text{C]} * \text{Power Level [\%]}_{26,0 100} \\
 & - 2,553 \text{ Temperature [}^\circ\text{C]} * \text{Power Level [\%]}_{30,0 50} \\
 & - 0,328 \text{ Temperature [}^\circ\text{C]} * \text{Power Level [\%]}_{30,0 75} \\
 & + 2,881 \text{ Temperature [}^\circ\text{C]} * \text{Power Level [\%]}_{30,0 100} \\
 & - 0,486 \text{ Temperature [}^\circ\text{C]} * \text{Water Tight}_{22,5 \text{ No}} \\
 & + 0,486 \text{ Temperature [}^\circ\text{C]} * \text{Water Tight}_{22,5 \text{ Yes}} \\
 & - 0,378 \text{ Temperature [}^\circ\text{C]} * \text{Water Tight}_{26,0 \text{ No}} \\
 & + 0,378 \text{ Temperature [}^\circ\text{C]} * \text{Water Tight}_{26,0 \text{ Yes}} \\
 & + 0,864 \text{ Temperature [}^\circ\text{C]} * \text{Water Tight}_{30,0 \text{ No}} \\
 & - 0,864 \text{ Temperature [}^\circ\text{C]} * \text{Water Tight}_{30,0 \text{ Yes}} \\
 & + 0,947 \text{ Power Level [\%]} * \text{Water Tight}_{50 \text{ No}} \\
 & - 0,947 \text{ Power Level [\%]} * \text{Water Tight}_{50 \text{ Yes}} \\
 & - 0,594 \text{ Power Level [\%]} * \text{Water Tight}_{75 \text{ No}} \\
 & + 0,594 \text{ Power Level [\%]} * \text{Water Tight}_{75 \text{ Yes}} \\
 & - 0,353 \text{ Power Level [\%]} * \text{Water Tight}_{100 \text{ No}} \\
 & + 0,353 \text{ Power Level [\%]} * \text{Water Tight}_{100 \text{ Yes}} \\
 & - 0,464 \text{ Temperature [}^\circ\text{C]} * \text{Power Level [\%]} * \text{Water Tight}_{22,5 50 \text{ No}} \\
 & + 0,464 \text{ Temperature [}^\circ\text{C]} * \text{Power Level [\%]} * \text{Water Tight}_{22,5 50 \text{ Yes}} \\
 & + 0,353 \text{ Temperature [}^\circ\text{C]} * \text{Power Level [\%]} * \text{Water Tight}_{22,5 75 \text{ No}} \\
 & - 0,353 \text{ Temperature [}^\circ\text{C]} * \text{Power Level [\%]} * \text{Water Tight}_{22,5 75 \text{ Yes}} \\
 & + 0,111 \text{ Temperature [}^\circ\text{C]} * \text{Power Level [\%]} * \text{Water Tight}_{22,5 100 \text{ No}} \\
 & - 0,111 \text{ Temperature [}^\circ\text{C]} * \text{Power Level [\%]} * \text{Water Tight}_{22,5 100 \text{ Yes}} \\
 & + 1,328 \text{ Temperature [}^\circ\text{C]} * \text{Power Level [\%]} * \text{Water Tight}_{26,0 50 \text{ No}} \\
 & - 1,328 \text{ Temperature [}^\circ\text{C]} * \text{Power Level [\%]} * \text{Water Tight}_{26,0 50 \text{ Yes}} \\
 & - 1,031 \text{ Temperature [}^\circ\text{C]} * \text{Power Level [\%]} * \text{Water Tight}_{26,0 75 \text{ No}} \\
 & + 1,031 \text{ Temperature [}^\circ\text{C]} * \text{Power Level [\%]} * \text{Water Tight}_{26,0 75 \text{ Yes}} \\
 & - 0,297 \text{ Temperature [}^\circ\text{C]} * \text{Power Level [\%]} * \text{Water Tight}_{26,0 100 \text{ No}} \\
 & + 0,297 \text{ Temperature [}^\circ\text{C]} * \text{Power Level [\%]} * \text{Water Tight}_{26,0 100 \text{ Yes}} \\
 & - 0,864 \text{ Temperature [}^\circ\text{C]} * \text{Power Level [\%]} * \text{Water Tight}_{30,0 50 \text{ No}} \\
 & + 0,864 \text{ Temperature [}^\circ\text{C]} * \text{Power Level [\%]} * \text{Water Tight}_{30,0 50 \text{ Yes}} \\
 & + 0,678 \text{ Temperature [}^\circ\text{C]} * \text{Power Level [\%]} * \text{Water Tight}_{30,0 75 \text{ No}} \\
 & - 0,678 \text{ Temperature [}^\circ\text{C]} * \text{Power Level [\%]} * \text{Water Tight}_{30,0 75 \text{ Yes}} \\
 & + 0,186 \text{ Temperature [}^\circ\text{C]} * \text{Power Level [\%]} * \text{Water Tight}_{30,0 100 \text{ No}} \\
 & - 0,186 \text{ Temperature [}^\circ\text{C]} * \text{Power Level [\%]} * \text{Water Tight}_{30,0 100 \text{ Yes}}
 \end{aligned}$$

Fits and Diagnostics for Unusual Observations

Obs	Pressure	Fit	Resid	Std Resid	
22	235,70	232,00	3,70	2,49	R
25	228,30	232,00	-3,70	-2,49	R
26	379,00	382,20	-3,20	-2,15	R
36	385,40	382,20	3,20	2,15	R

R Large residual



A.8 DOE - 2k Factorial Design Result

EXP. 1 - 2K FACTORIAL

Factorial Regression: Pressure versus Temperature [°C]; Power Level [%]; Water Tight

Coded Coefficients

Term	Effect	Coef	SE Coef	T-Value	P-Value	VIF
Constant		425,131	0,373	1140,52	0,000	
Temprature [°C]	8,612	4,306	0,373	11,55	0,000	1,00
Power Level [%]	92,288	46,144	0,373	123,79	0,000	1,00
Water Tight	3,488	1,744	0,373	4,68	0,002	1,00
Temprature [°C]*Power Level [%]	2,837	1,419	0,373	3,81	0,005	1,00
Temprature [°C]*Water Tight	0,788	0,394	0,373	1,06	0,322	1,00
Power Level [%]*Water Tight	-0,487	-0,244	0,373	-0,65	0,532	1,00
Temprature [°C]*Power Level [%]*Water Tight	-0,487	-0,244	0,373	-0,65	0,532	1,00

Model Summary

S	R-sq	R-sq(adj)	R-sq(pred)
1,49101	99,95%	99,90%	99,79%

Analysis of Variance

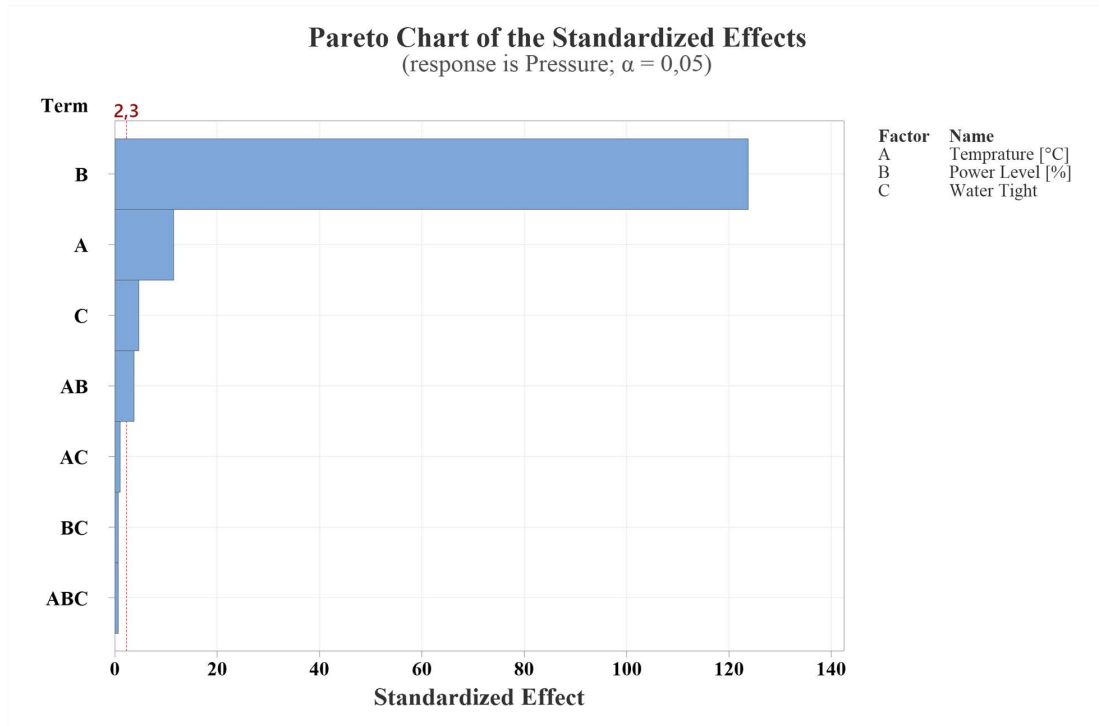
Source	DF	Adj SS	Adj MS	F-Value	P-Value
Model	7	34449,9	4921,4	2213,74	0,000
Linear	3	34413,3	11471,1	5159,90	0,000
Temprature [°C]	1	296,7	296,7	133,46	0,000
Power Level [%]	1	34067,9	34067,9	15324,34	0,000
Water Tight	1	48,7	48,7	21,88	0,002
2-Way Interactions	3	35,6	11,9	5,34	0,026
Temprature [°C]*Power Level [%]	1	32,2	32,2	14,49	0,005
Temprature [°C]*Water Tight	1	2,5	2,5	1,12	0,322
Power Level [%]*Water Tight	1	1,0	1,0	0,43	0,532
3-Way Interactions	1	1,0	1,0	0,43	0,532
Temprature [°C]*Power Level [%]*Water Tight	1	1,0	1,0	0,43	0,532
Error	8	17,8	2,2		
Total	15	34467,7			

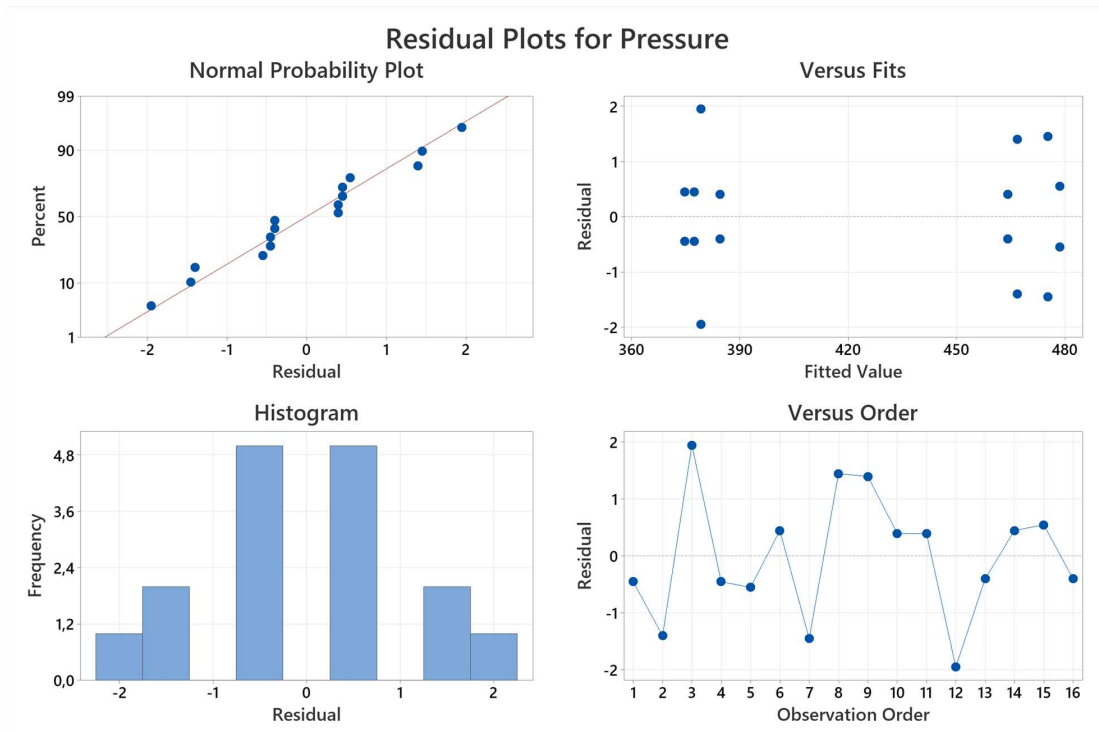
Regression Equation in Uncoded Units

$$\begin{aligned} \text{Pressure} = & 180,1 - 3,21 \text{ Temperature } [^{\circ}\text{C}] + 2,119 \text{ Power Level } [\%] \\ & - 25,6 \text{ Water Tight} \\ & + 0,0649 \text{ Temperature } [^{\circ}\text{C}] * \text{Power Level } [\%] \\ & + 1,20 \text{ Temperature } [^{\circ}\text{C}] * \text{Water Tight} \\ & + 0,251 \text{ Power Level } [\%] * \text{Water Tight} \\ & - 0,0111 \text{ Temperature } [^{\circ}\text{C}] * \text{Power Level } [\%] * \text{Water Tight} \end{aligned}$$

Alias Structure

Factor	Name
A	Temperature [°C]
B	Power Level [%]
C	Water Tight





DEPARTMENT OF INDUSTRIAL AND MATERIAL SCIENCE
CHALMERS UNIVERSITY OF TECHNOLOGY

Gothenburg, Sweden

www.chalmers.se



CHALMERS
UNIVERSITY OF TECHNOLOGY